Università degli Studi di Pavia
Facoltà di Ingegneria
PhD Program in Design, Modeling, and Simulation in Engineering
XXXIII ciclo

Advanced isogeometric methods with a focus on composite laminated structures

Alessia Patton

Pavia, April 20, 2021

Supervisor:
Prof. Alessandro Reali

Co-supervisor:
Dr. Guillermo Lorenzo

Motivation

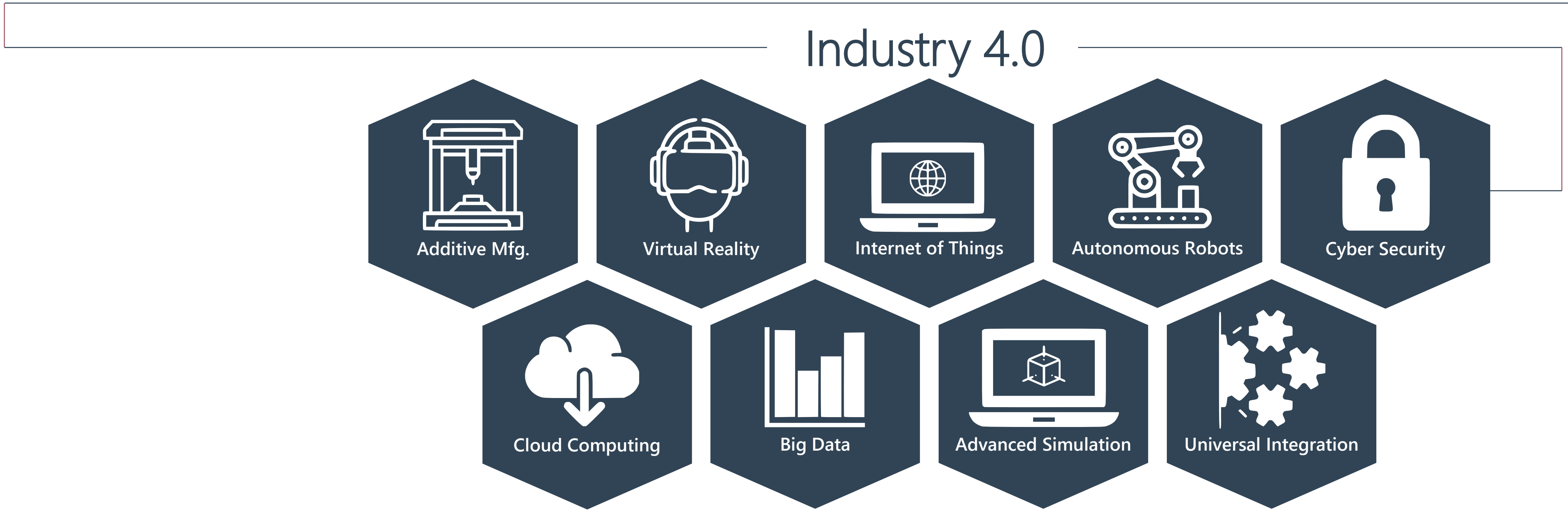
Industry 4.0
Additive Mfg.
Virtual Reality
Internet of Things
Autonomous Robots
Cyber Security
Cloud Computing
Big Data
Advanced Simulation
Universal Integration

Motivation

Industry 4.0

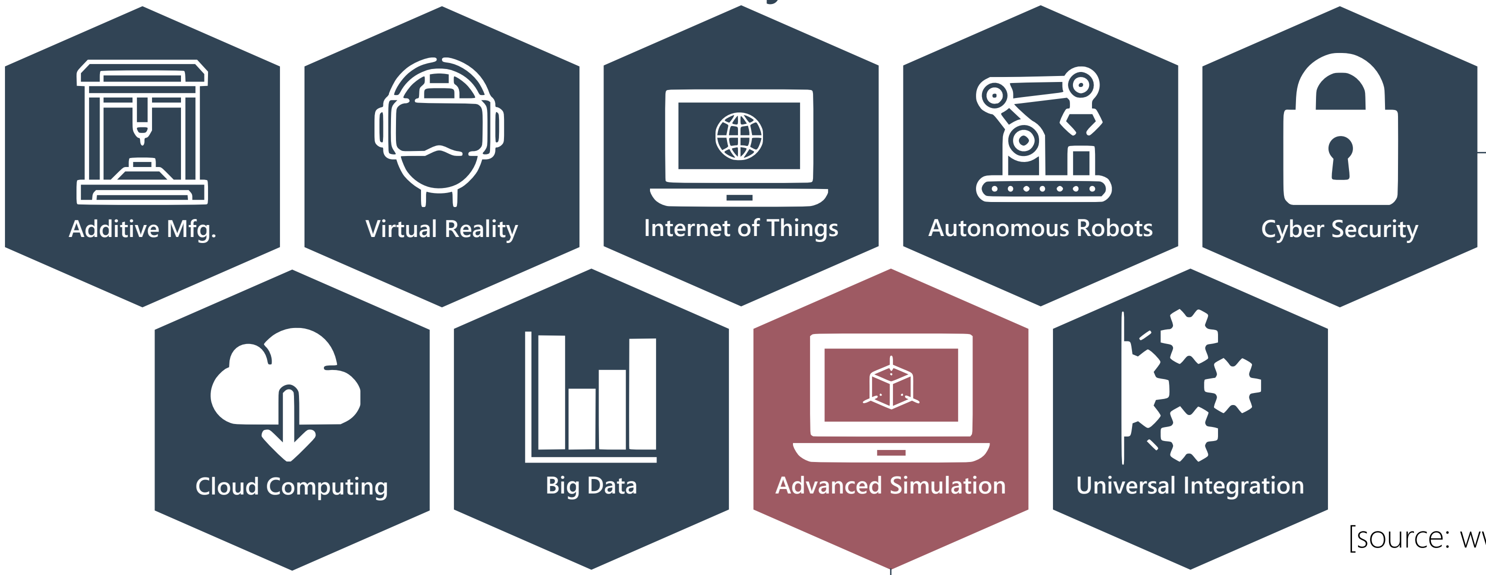

[source: www.cis.tennessee.edu]

Why Advanced Simulation modeling?

- risk-free environment
- save money and time
- increased accuracy
- visualization

[source: www.anylogic.com; www.smactory.com]

Outline

- Motivation
- Cost-effective IgA strategies to model composite structures
- An explicit algorithm for irreversibility enforcement in phase-field modeling of crack propagation
- Towards novel IgA methods for fluid-structure interaction problems
- Conclusions and Future works

Outline

- Motivation
- Cost-effective IgA strategies to model composite structures
- An explicit algorithm for irreversibility enforcement in phase-field modeling of crack propagation
- Towards novel IgA methods for fluid-structure interaction problems
- Conclusions and Future works

Background

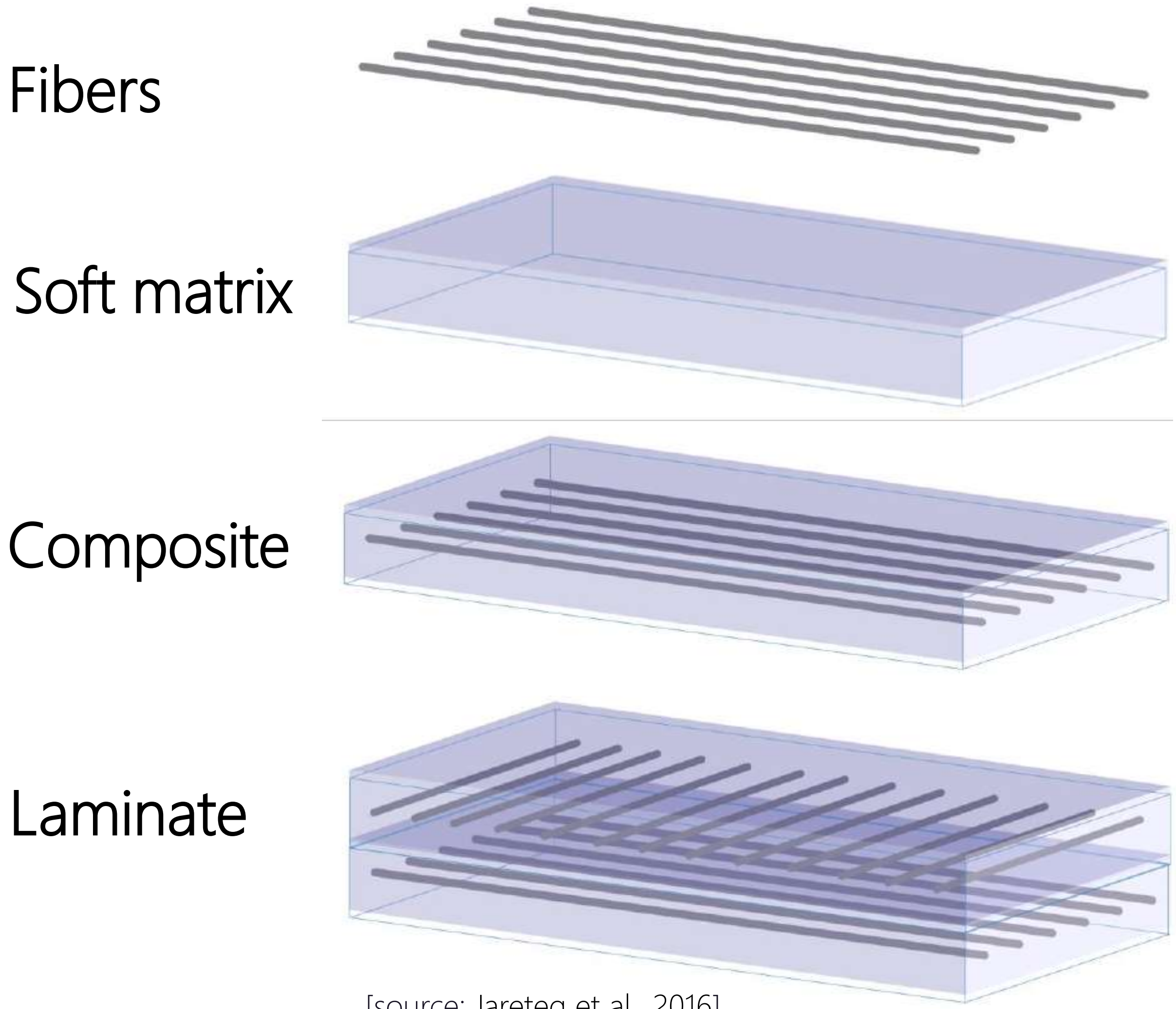

[source: Jareteg et al., 2016]

- design flexibility
- light weight
- high strength and stiffness
- corrosion resistance
- durability

[source: www.performancecomposites.com]

Motivation

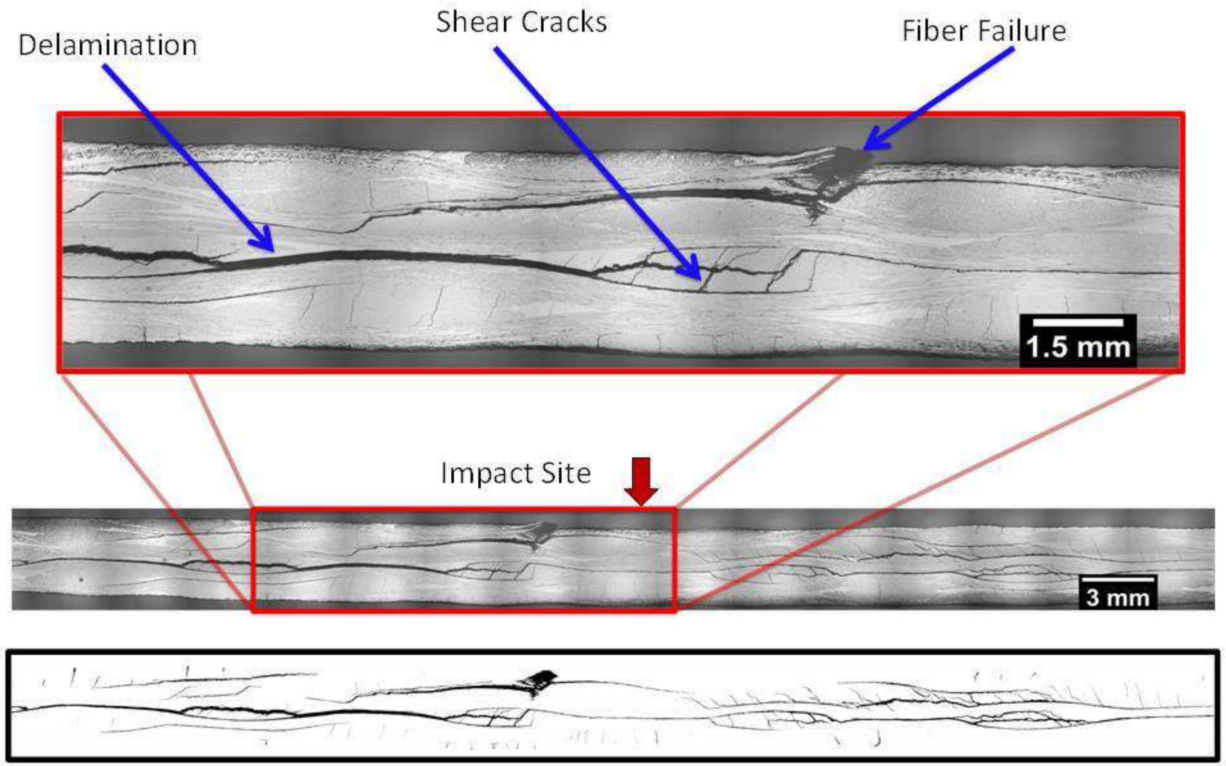

[source: http://kevinrhart.com]

Understanding composites **failure modes** and **complex behavior** is **essential** for **designing purposes** and requires knowledge of the **whole 3D stress state**

Motivation

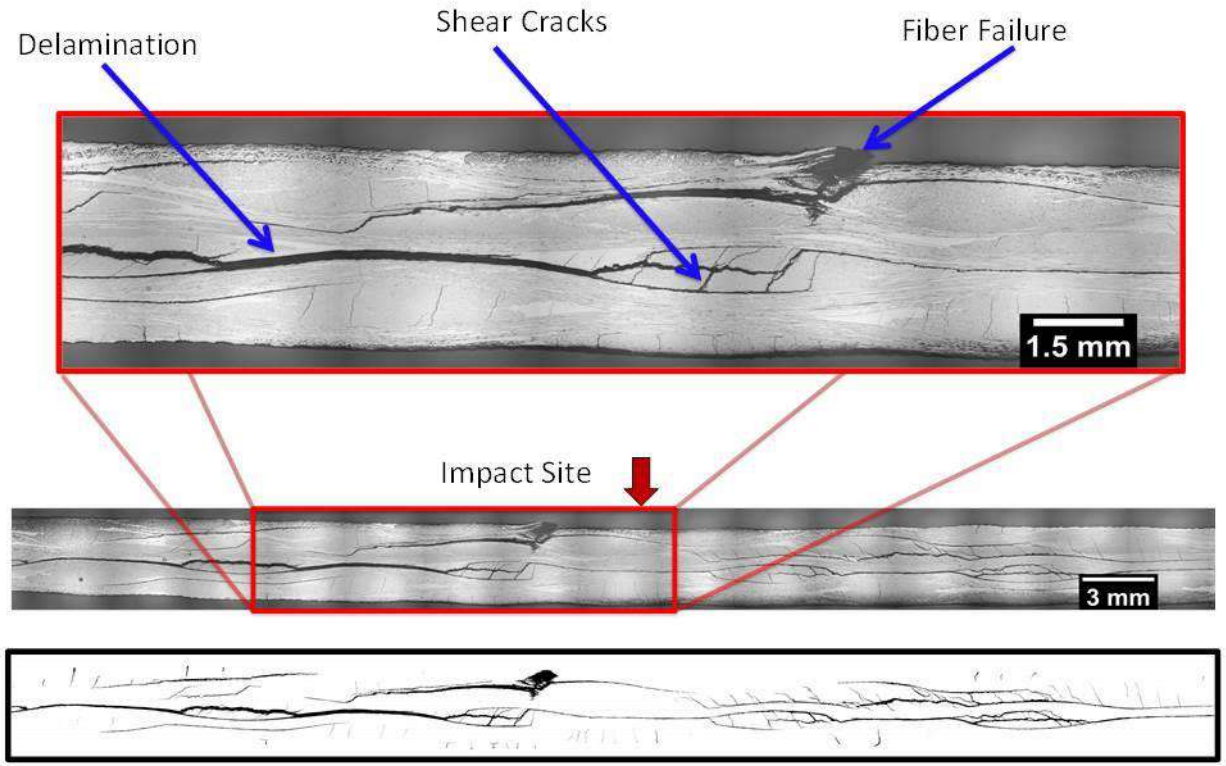

[source: http://kevinrhart.com]

Objective: Inexpensive simulations able to accurately predict the 3D stress state for stacks with a significant number of layers

Modeling strategy

Exploit Isogeometric Analysis (IgA, Hughes et al., 2005) high-order continuity properties and typically excellent accuracy-to computational-effort ratio

IgA Galerkin approaches (IgG)

[Hughes, Cottrell, Bazilevs, CMAME 2005]

Alternative to standard FE analysis (based on typical CAD basis functions, e.g., NURBS), *including isoparametric FEA as a special case*, but offering other possibilities:

- ✓ precise and efficient geometric modeling
- ✓ smooth basis functions with compact support
- ✓ simplified mesh refinement
- ✓ superior approximation properties
- ✓ integration of design and analysis

IgA collocation methods (IgC)

[Auricchio, Beirão da Veiga, Hughes, Reali, Sangalli, M3AS 2010]

Approximation performed through direct evaluation of the differential equations governing the problem at suitable points [*no integrals to compute!*]

- ✓ easy implementation (e.g., isoparametric concept adoption; discrete differential equations evaluation in *strong form* at each collocation point)
- ✓ fast method (in terms of *evaluation* and *assembly operations*)
- ✓ high orders of convergence

Modeling strategy

Exploit Isogeometric Analysis (IgA, Hughes et al., 2005) high-order continuity properties and typically excellent accuracy-to computational-effort ratio

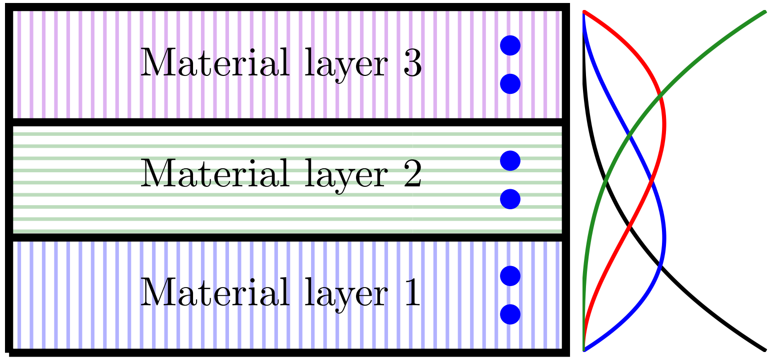

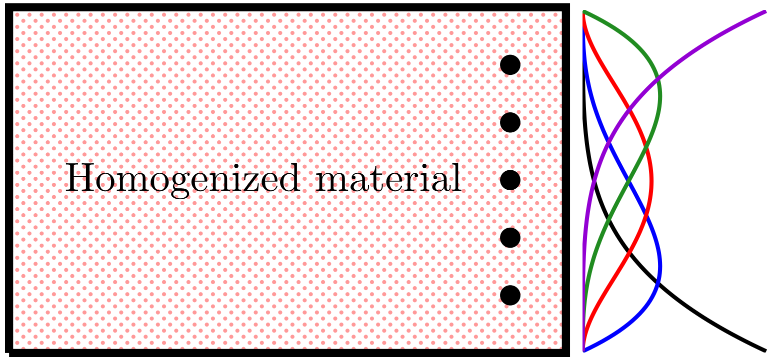

[Sun et al., IJCM 1988]

Single-element approach

- ✓ accurate displacements
- ✓ accurate in-plane stresses
- × inaccurate out-of-plane stresses
- ✓ inexpensive (in particular for a significant number of layers)

Remarks:

- Ad hoc through-the-thickness integration rule (i.e., r - 1 Gauss points per layer, being r the out-of-plane degree of approximation) for IgG
- Homogenized approach and r + 1 evaluation points independently on the number of layers for IgC

Through-the-thickness solution

The use of a single element through the thickness with highly continuous shape functions leads to an accurate in-plane stress solution

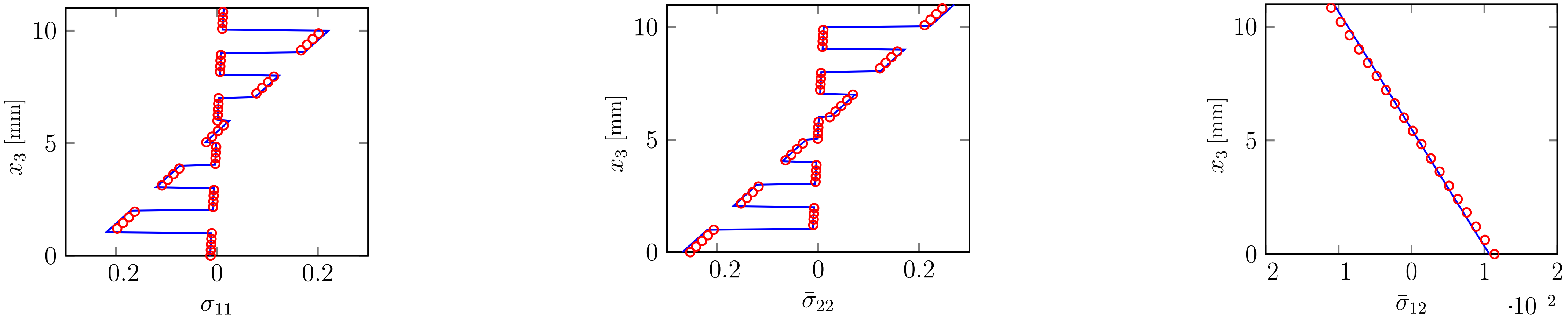

This is not the case for the out-of-plane stress state

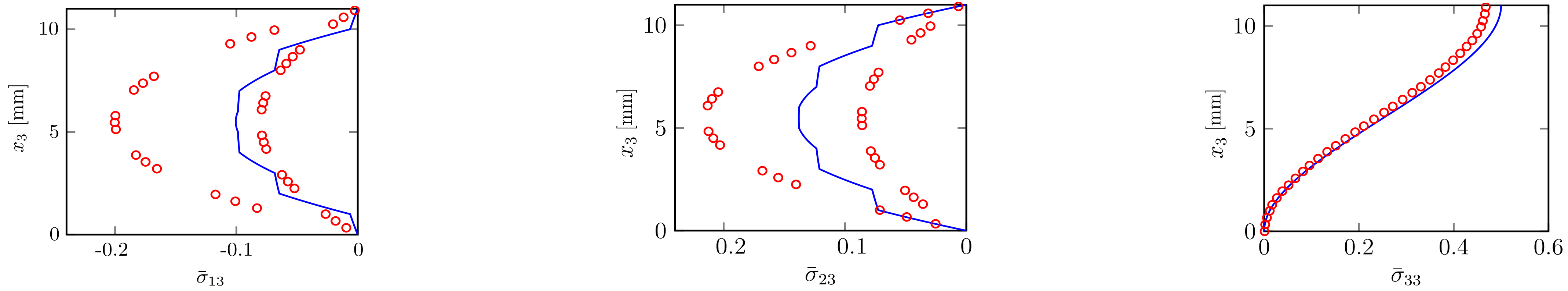

S=50, 11 layers (— Pagano's solution, ○ IgA-Collocation with p=q=6, r=4, and 10x10x5 collocation points)

The Equilibrium-based post-processing technique

Problem: The single-element approach guarantees inexpensive simulations (in particular for a significant number of layers), but is inaccurate in predicting out-of-plane stresses (fundamental for delamination)

Directly recover an **accurate out-of-plane stress state** from **equilibrium** at locations of interest

$$\nabla \cdot \boldsymbol{\sigma} + \mathbf{b} = \mathbf{0}$$

Key ingredients for stress recovery effectiveness are granted by IgA properties!

- ✓ accurate in-plane solution (even with a coarse mesh)
- ✓ accurate derivatives of in-plane stresses (high-order continuity of the displacement field)

The Equilibrium-based post-processing technique

Problem: The single-element approach guarantees inexpensive simulations (in particular for a significant number of layers), but is inaccurate in predicting out-of-plane stresses (fundamental for delamination)

Directly recover an accurate out-of-plane stress state from equilibrium at locations of interest

$$\sigma_{11,1} + \sigma_{12,2} + \sigma_{13,3} = b_1$$

$$\sigma_{12,1} + \sigma_{22,2} + \sigma_{23,3} = b_2$$

$$\sigma_{13,1} + \sigma_{23,2} + \sigma_{33,3} = b_3$$

Key ingredients for stress recovery effectiveness are granted by IgA properties!

- ✓ accurate in-plane solution (even with a coarse mesh)
- ✓ accurate derivatives of in-plane stresses (high-order continuity of the displacement field)

The Equilibrium-based post-processing technique

Problem: The single-element approach guarantees inexpensive simulations (in particular for a significant number of layers), but is inaccurate in predicting out-of-plane stresses (fundamental for delamination)

Directly recover an accurate out-of-plane stress state from equilibrium at locations of interest

$$\underbrace{\sigma_{11,1} + \sigma_{12,2}}_{\text{well approximated}} + \sigma_{13,3} = b_1$$

$$\underbrace{\sigma_{12,1} + \sigma_{22,2}}_{\text{well approximated}} + \sigma_{23,3} = b_2$$

$$\sigma_{13,1} + \sigma_{23,2} + \sigma_{33,3} = b_3$$

Key ingredients for stress recovery effectiveness are granted by IgA properties!

- ✓ accurate in-plane solution (even with a coarse mesh)
- ✓ accurate derivatives of in-plane stresses (high-order continuity of the displacement field)

The Equilibrium-based post-processing technique

Problem: The single-element approach guarantees inexpensive simulations (in particular for a significant number of layers), but is inaccurate in predicting out-of-plane stresses (fundamental for delamination)

Directly recover an accurate out-of-plane stress state from equilibrium at locations of interest

$$\underbrace{\sigma_{11,1} + \sigma_{12,2}}_{\text{well approximated}} + \underbrace{\sigma_{13,3}}_{\text{recovered}} = b_1$$

$$\underbrace{\sigma_{12,1} + \sigma_{22,2}}_{\text{well approximated}} + \underbrace{\sigma_{23,3}}_{\text{recovered}} = b_2$$

$$\underbrace{\sigma_{13,1} + \sigma_{23,2}}_{\text{recovered}} + \underbrace{\sigma_{33,3}}_{\text{recovered}} = b_3$$

Key ingredients for stress recovery effectiveness are granted by IgA properties!

- ✓ accurate in-plane solution (even with a coarse mesh)
- ✓ accurate derivatives of in-plane stresses (high-order continuity of the displacement field)

The Equilibrium-based post-processing technique

Directly recover an accurate out-of-plane stress state
from **equilibrium** at locations of interest

$$\sigma_{13}(x_3) = -\int_{\bar{x}_3}^{x_3} \big(\sigma_{11,1}(\zeta) + \sigma_{12,2}(\zeta) - b_1(\zeta)\big)\mathrm{d}\zeta + \sigma_{13}(\bar{x}_3)$$

$$\sigma_{23}(x_3) = -\int_{\bar{x}_3}^{x_3} \big(\sigma_{12,1}(\zeta) + \sigma_{22,2}(\zeta) - b_2(\zeta)\big)\mathrm{d}\zeta + \sigma_{23}(\bar{x}_3)$$

$$\begin{aligned}\sigma_{33}(x_3) = \int_{\bar{x}_3}^{x_3} \Bigg[\int_{\bar{x}_3}^{\zeta} &\big(\sigma_{11,11}(\xi) + \sigma_{22,22}(\xi) + 2\sigma_{12,12}(\xi) \\ &- b_{1,1}(\xi) - b_{2,2}(\xi)\big)\mathrm{d}\xi\Bigg]\mathrm{d}\zeta + \int_{\bar{x}_3}^{x_3} b_3(\zeta)\mathrm{d}\zeta \\ &+ (\bar{x}_3 - x_3)\big(\sigma_{13,1}(\bar{x}_3) + \sigma_{23,2}(\bar{x}_3)\big) + \sigma_{33}(\bar{x}_3)\end{aligned}$$

IgA single-element approach
+
Equilibrium-based post-processing

- ✓ accurate displacements
- ✓ accurate in-plane stresses
- ✓ accurate derivatives of in-plane stresses
- ✓ accurate out-of-plane stresses
- ✓ inexpensive (in particular for a significant number of layers)

The post-processing effect

After the post-processing step is applied, an accurate out-of-plane stress solution is recovered, retrieving what is prescribed by equilibrium

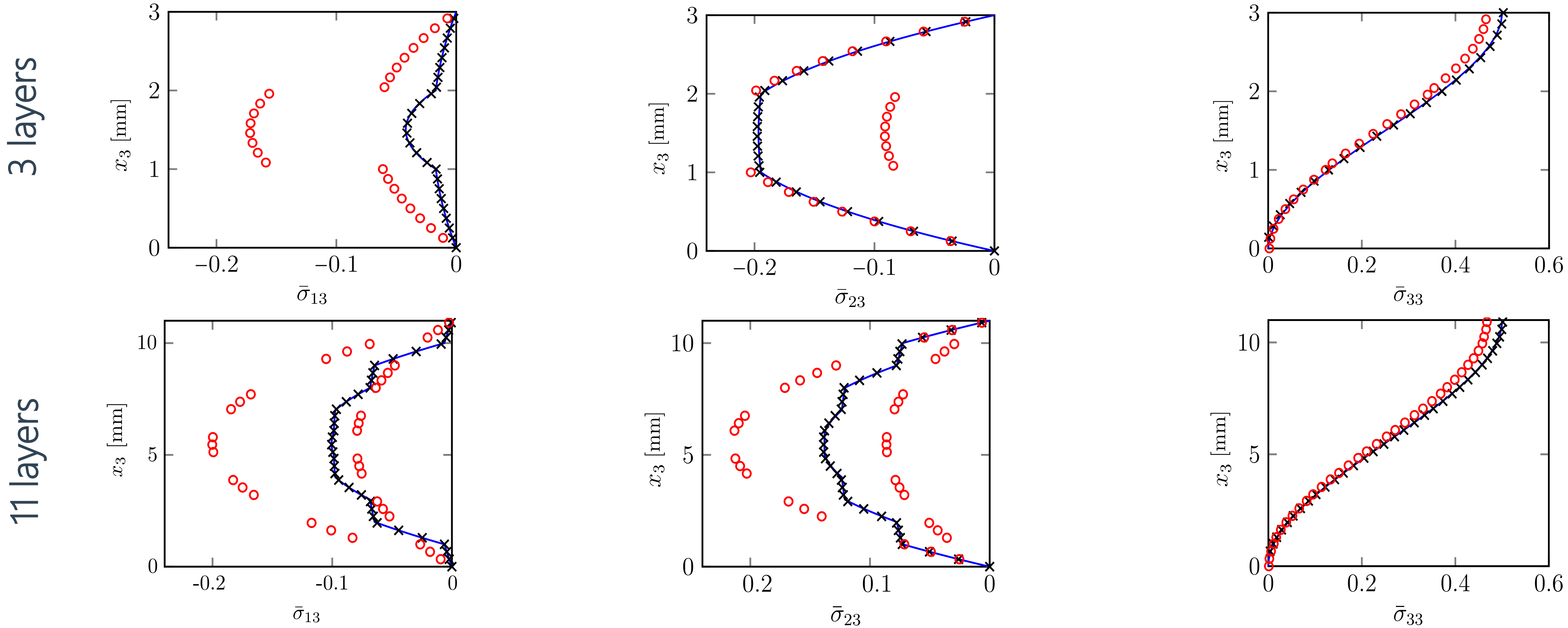

S=50 (— Pagano's solution. ○ IgC without post-processing, and × post-processed IgC with p=q=6, r=4, and 10x10x5 collocation points)

Parametric study on length-to-thickness ratio

3 layers

33 layers

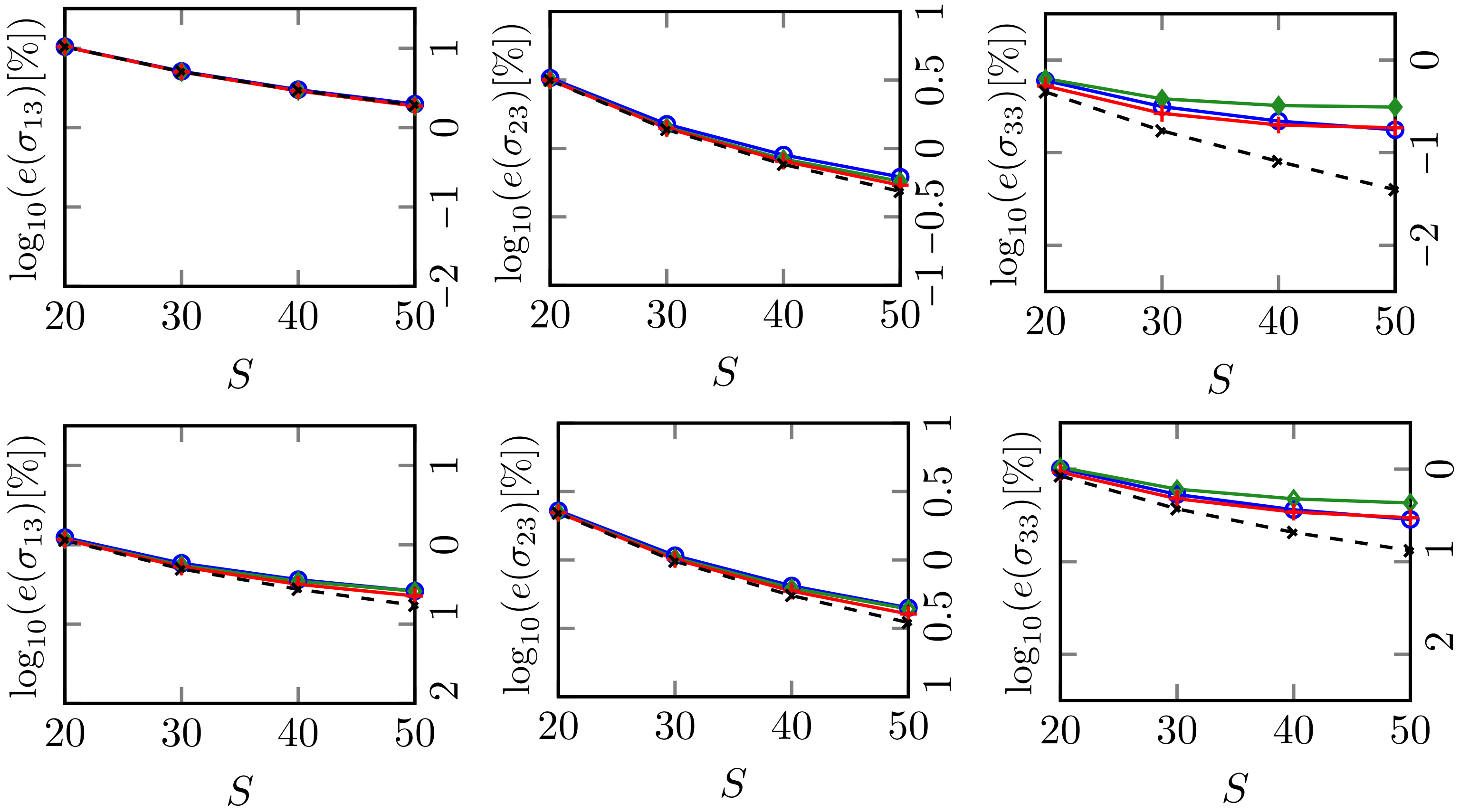

post-processed IgC with p=q=6, r=4, and 10x10x5 collocation points (○ 1 knot span, ♦ 2 knot spans, + 4 knot spans, × 8 knot spans)

- ✓ even very coarse in-plane meshes yield to accurate results
- ✓ the higher the number of layers and thinner the plate, the better the approximation
- ✓ maximum percentage errors of 1% or lower using only one element of degrees p = q = 6, r = 4 (for 11 and 33 layers, S≥30)

AP, J.-E. Dufour, P. Antolin, and A. Reali, Fast and accurate elastic analysis of laminated composite plates via isogeometric collocation and an equilibrium-based stress recovery approach, *Composite Structures* (2019) 225: 111026.

Extension to bivariate Kirchhoff plates

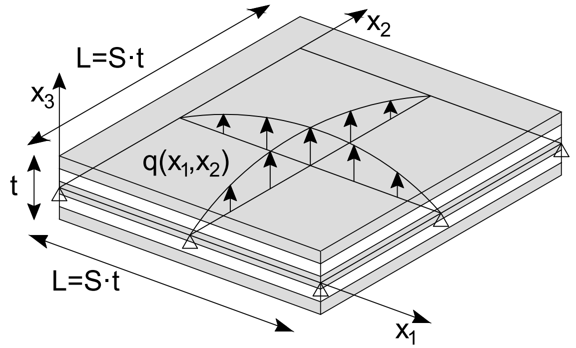

- displacement-based CLPT approach
- Hyp: multiple specially orthotropic layers
- homogenized material properties with exact integration along the thickness

IgA single-element approach

- ✓ accurate displacements
- ✓ accurate in-plane stresses
- ✗ zero out-of-plane stresses considering Kirchhoff plate CLPT formulation
- ✓ accurate derivatives of in-plane stresses

$$\sigma_{13}(x_3) = -\int_{\bar{x}_3}^{x_3} \left(\sigma_{11,1}(\zeta) + \sigma_{12,2}(\zeta) - b_1(\zeta)\right)\mathrm{d}\zeta + \sigma_{13}(\bar{x}_3)$$

$$\sigma_{23}(x_3) = -\int_{\bar{x}_3}^{x_3} \left(\sigma_{12,1}(\zeta) + \sigma_{22,2}(\zeta) - b_2(\zeta)\right)\mathrm{d}\zeta + \sigma_{23}(\bar{x}_3)$$

$$\sigma_{33}(x_3) = \int_{\bar{x}_3}^{x_3} \left[\int_{\bar{x}_3}^{\zeta} \left(\sigma_{11,11}(\xi) + \sigma_{22,22}(\xi) + 2\sigma_{12,12}(\xi) - b_{1,1}(\xi) - b_{2,2}(\xi)\right)\mathrm{d}\xi\right]\mathrm{d}\zeta + \int_{\bar{x}_3}^{x_3} b_3(\zeta)\mathrm{d}\zeta + (\bar{x}_3 - x_3)\left(\sigma_{13,1}(\bar{x}_3) + \sigma_{23,2}(\bar{x}_3)\right) + \sigma_{33}(\bar{x}_3)$$

\+

Equilibrium-based post-processing

- ✓ accurate out-of-plane stresses

Note: the post-processing within the Kirchhoff plate formulation demands higher regularity w.r.t. the solid plate modeling (i.e., C^3-continuity easily achieved *via* IgA!)

$$\begin{cases} \sigma_{\alpha\beta,\gamma} = \mathbb{C}_{\alpha\beta\zeta\eta}(x_3)(-x_3\kappa_{\zeta\eta,\gamma}) = \mathbb{C}_{\alpha\beta\zeta\eta}(x_3)(-x_3 w_{,\zeta\eta\gamma}) \\ \sigma_{\alpha\beta,\gamma\delta} = \mathbb{C}_{\alpha\beta\zeta\eta}(x_3)(-x_3\kappa_{\zeta\eta,\gamma\delta}) = \mathbb{C}_{\alpha\beta\zeta\eta}(x_3)(-x_3 w_{,\zeta\eta\gamma\delta}) \end{cases}$$

Numerical Validation

Pagano testcase

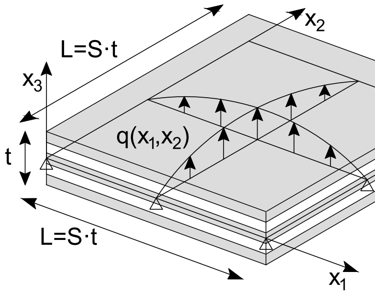

✓ Possible to model unsymmetrical layer stacks also for collocation

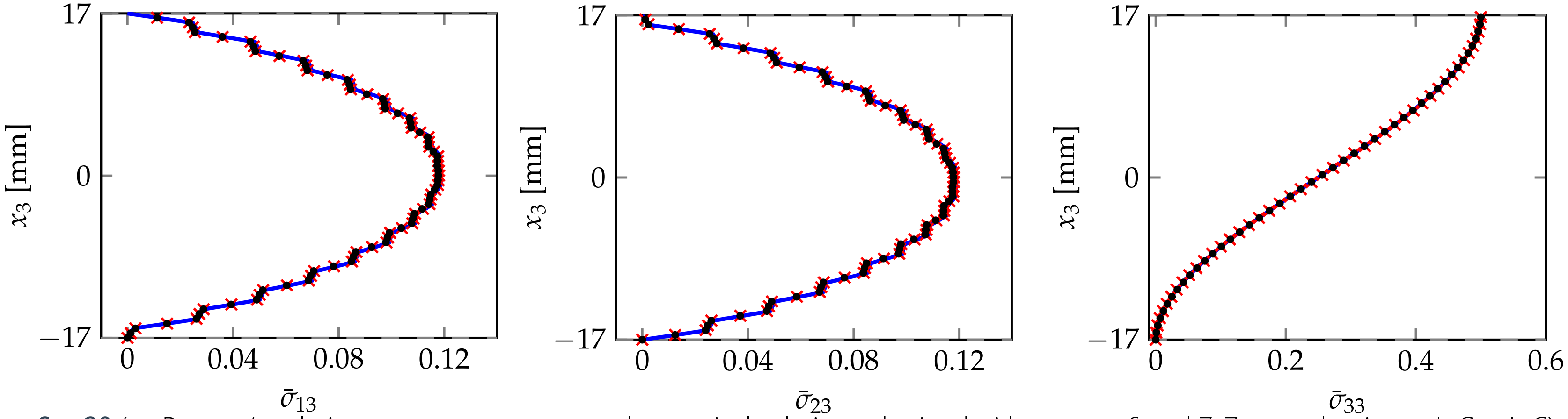

S = 20 (▬ Pagano's solution, versus post-processed numerical solutions obtained with p = q = 6 and 7x7 control points: × IgG, • IgC)

Simply supported circular plate subject to a uniformly distributed load

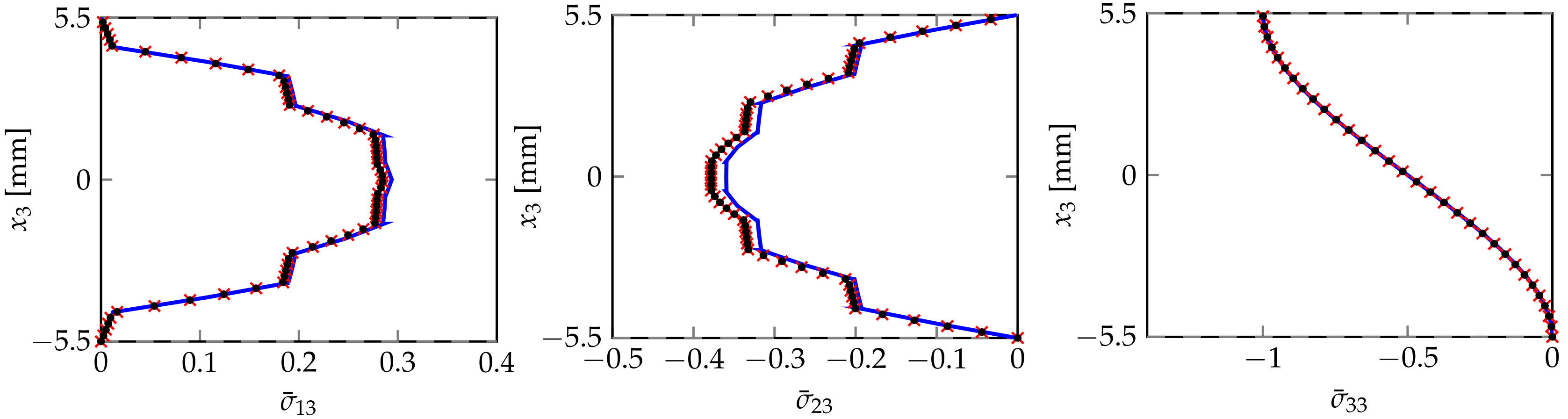

mean radius-to-thickness ratio S = 20 (▬ overkill Abaqus Unified FEA solution with 466,136 C3D20R finite elements versus post-processed numerical solutions obtained with p=q=6 and 14x14 control points: × IgG, • IgC)

- Remark: higher interelement continuity may be of key importance simulating more complex geometrical features

AP, P. Antolin, J.-E. Dufour, J. Kiendl, and A. Reali, Accurate equilibrium-based interlaminar stress recovery for isogeometric laminated composite Kirchhoff plates, *Composite Structures* (2021) 256: 112976.

Extension to solid shells

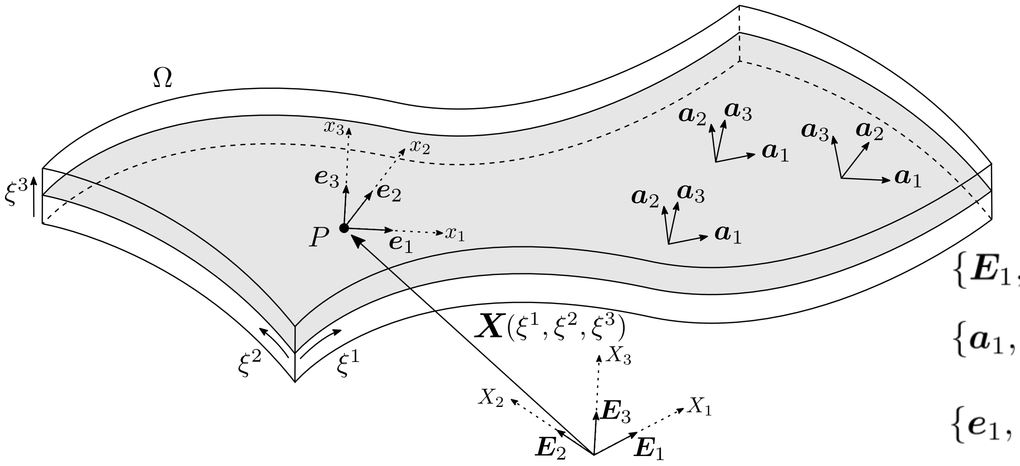

$\{\boldsymbol{E}_1, \boldsymbol{E}_2, \boldsymbol{E}_3\}$ Global basis

$\{\boldsymbol{a}_1, \boldsymbol{a}_2, \boldsymbol{a}_3\}$ Local orthonormal moving basis

$\{\boldsymbol{e}_1, \boldsymbol{e}_2, \boldsymbol{e}_3\}$ Fixed local orthonormal basis

Compute the displacement solution in the global reference system and perform the stress-recovery locally

$$\sigma_{13}(x_3) = -\int_{\bar{x}_3}^{x_3} (\sigma_{11,1}(\zeta) + \sigma_{12,2}(\zeta) - b_1(\zeta))\mathrm{d}\zeta + \sigma_{13}(\bar{x}_3)$$

$$\sigma_{23}(x_3) = -\int_{\bar{x}_3}^{x_3} (\sigma_{12,1}(\zeta) + \sigma_{22,2}(\zeta) - b_2(\zeta))\mathrm{d}\zeta + \sigma_{23}(\bar{x}_3)$$

Numerical integration focused on the *k*-th layer

$$\sigma_{33,3}^{(k)}(x_3^{(k)}) = \int_{\underline{x}_3^{(k)}}^{x_3^{(k)}} (\sigma_{11,11}(\zeta) + \sigma_{22,22}(\zeta) + 2\sigma_{12,12}(\zeta) + b_{1,1}(\zeta) + b_{2,2}(\zeta))\mathrm{d}\zeta$$
$$- (\sigma_{13,1}(\underline{x}_3^{(k)}) + \sigma_{23,2}(\underline{x}_3^{(k)})) - b_3(x_3^{(k)})$$

$$\sigma_{33}(x_3) = \int_{\underline{x}_3}^{x_3} \sigma_{33,3}(\xi)\mathrm{d}\xi + \sigma_{33}(\underline{x}_3)$$

IgA single-element approach
+
Local Equilibrium-based post-processing

- ✓ accurate displacements
- ✓ accurate in-plane stresses
- ✓ accurate derivatives of in-plane stresses
- ✓ accurate out-of-plane stresses
- ✓ uncoupled equilibrium equations
- × more elaborated stress derivative terms

Extension to solid shells

Numerical validation

Hollow cylindrical solid shell under internal pressure

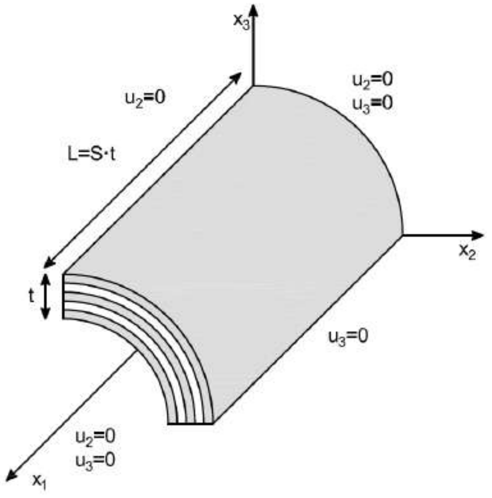

$q(x_1, x_2) = q_0 \cos(4\pi\theta) \sin(\frac{\pi x}{L})$

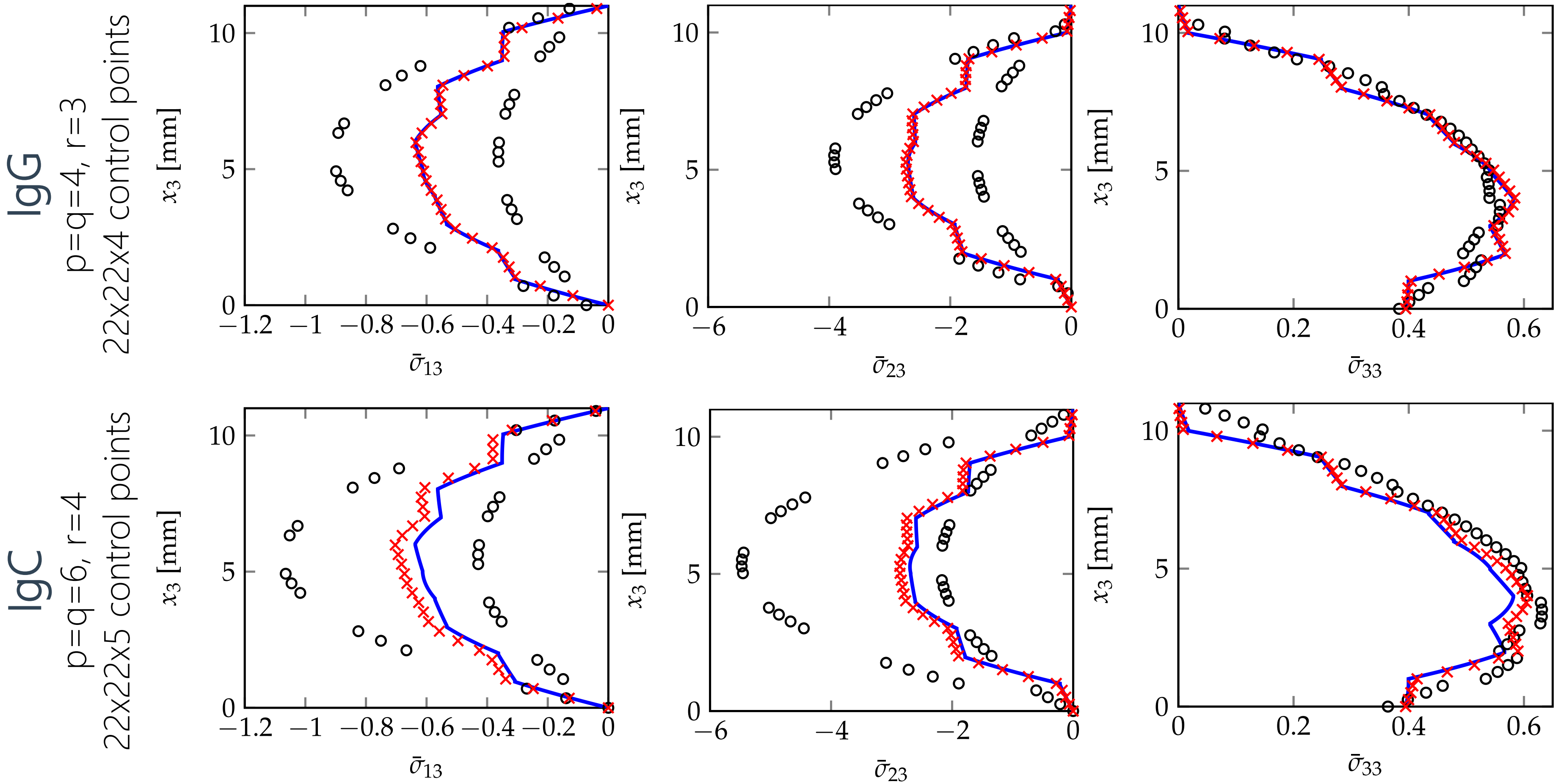

mean radius-to-thickness ratio S=20 (— overkill LW p=q=6, r=4 and 36x36x55 control points; × post-processed single-element solution, ○ single-element solution without post-processing)

Doubly-curved shells

Hemispherical solid shell with cut-outs under internal pressure

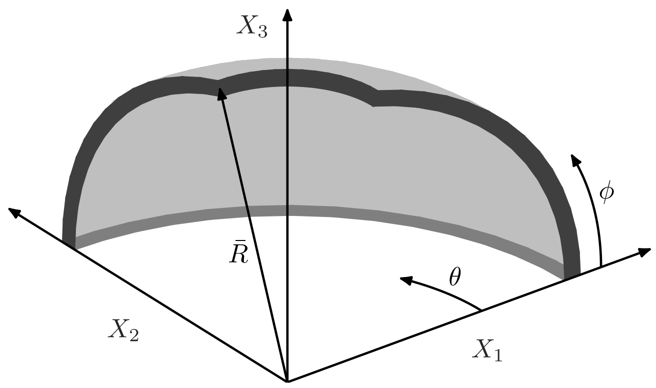

mean radius-to-thickness ratio S=20 (— overkill LW with p=q=6, r=4 and 36x36x55 control points; IgG with p=q=4, r=3 and 22x22x4 control points: × post-processed single-element; ○ single-element without post-processing)

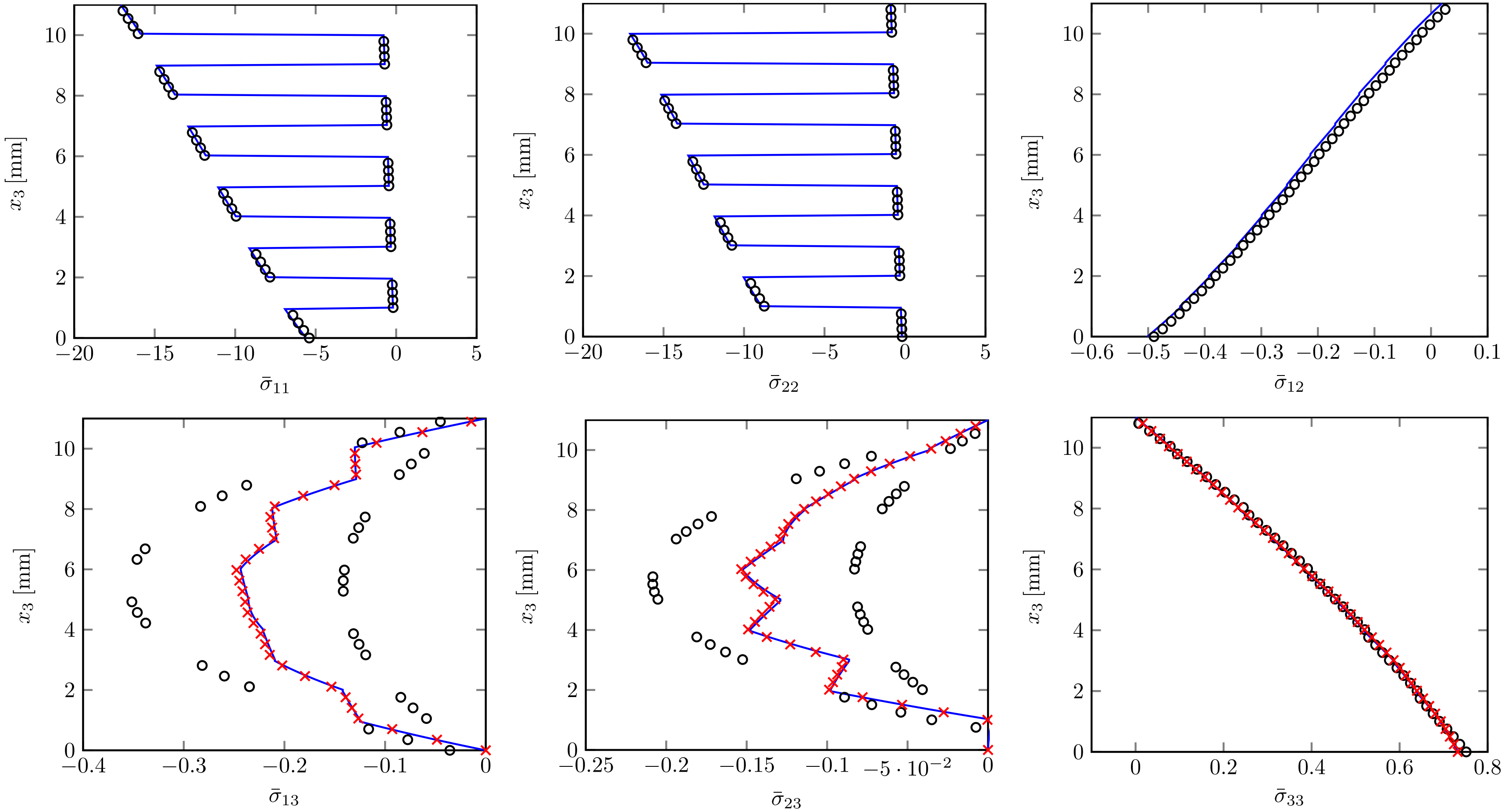

AP, P. Antolin, J. Kiendl, and A. Reali, Efficient equilibrium-based stress recovery for isogeometric laminated curved structures, accepted for publication on *Composite Structures*.

Outline

- Motivation
- Cost-effective IgA strategies to model composite structures
- An explicit algorithm for irreversibility enforcement in phase-field modeling of crack propagation
- Towards novel IgA methods for fluid-structure interaction problems
- Conclusions and Future works

Motivation

Computational challeges in phase-field modeling

non-convexity of the Total energy functional

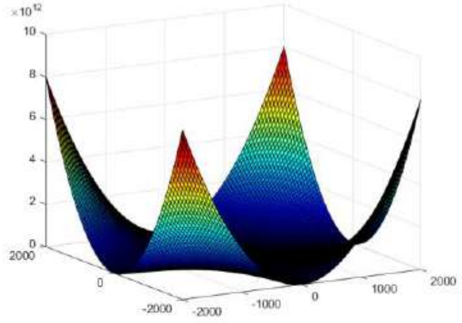

need to resolve small internal length l_0

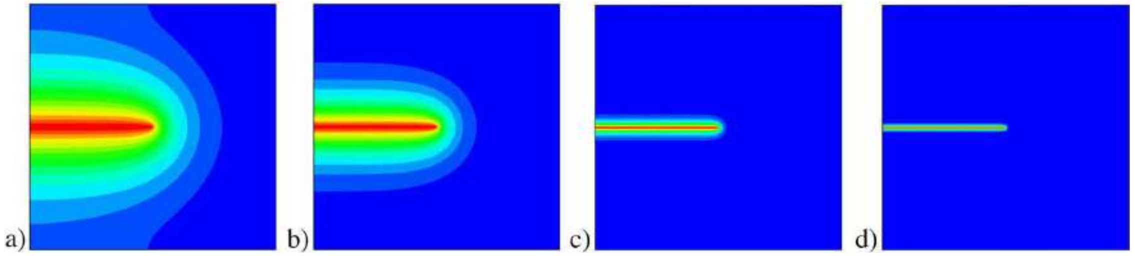

$l_0^{(a)} > l_0^{(b)} > l_0^{(c)} > l_0^{(d)}$ [Miehe et al., CMAME 2010]

irreversibility condition imposition on the phase-field $\dot{d} \geq 0$

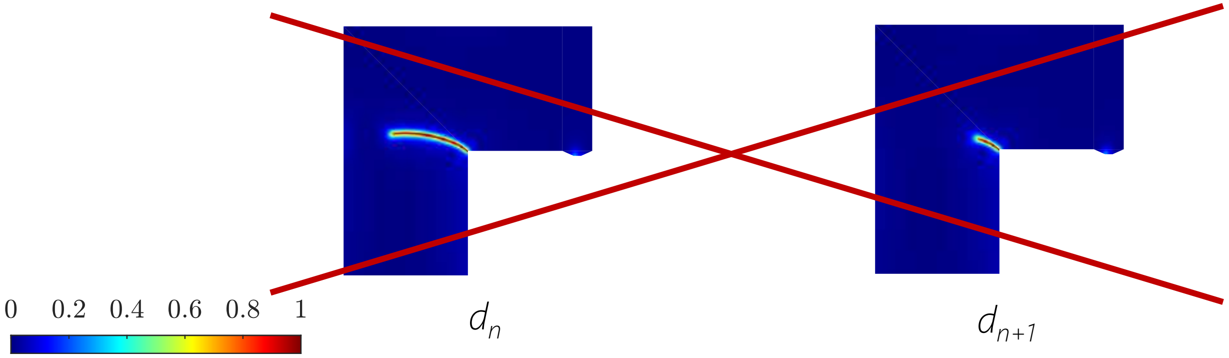

d_n d_{n+1}

Basics

BASICS OF THE MODEL

$$\Pi(\boldsymbol{u}, d) := \mathcal{E}(\boldsymbol{u}, d) + \boxed{G_c}\mathcal{D}(d) - \int_\Omega \boldsymbol{b}\cdot\boldsymbol{u}\,\mathrm{d}\Omega + \int_{\partial\Omega_N} \boldsymbol{t}\cdot\boldsymbol{u}\,\mathrm{d}\Gamma$$

CRITICAL FRACTURE ENERGY

ELASTIC ENERGY FUNCTIONAL

$$\mathcal{E}(\boldsymbol{u}, d) := \int_\Omega [\,\underbrace{(1-d)^2}(\psi_D + \psi_V^+) + \psi_V^-\,]\,\mathrm{d}\Omega$$

Positive/negative split of the elastic energy density [Amor et al., JMPS 2009]

$\omega = d^2$ AT2

PHASE-FIELD ENERGY FUNCTIONAL

$$\mathcal{D}(d) := \int_\Omega \frac{1}{2}(l_0^{-1}\boxed{d^2} + l_0|\boldsymbol{\nabla} d|^2)\,\mathrm{d}\Omega$$

BASICS OF ITS NUMERICAL IMPLEMENTATION

Algorithm 6.1 Staggered iteration algorithm.

input : load solution $(\boldsymbol{u}_n, d_n)$ from step n and boundary conditions $\boldsymbol{g}_{n+1}$, $\boldsymbol{t}_{n+1}$ at current step $n+1$

initialize $i = 0$

set $(\boldsymbol{u}^0, d^0) := (\boldsymbol{u}_n, d_n)$

while $Res_{stag} \geq \mathtt{TOL}_{stag}$ **do**

- $i \to i+1$
- given d^{i-1}, find $\boldsymbol{u}^i$ solving $\partial_u\Pi(\boldsymbol{u}^i, d^{i-1}) = \boldsymbol{0}$
- given $\boldsymbol{u}^i$, find d^i solving $\partial_d\Pi(\boldsymbol{u}^i, d^i)[\Delta d^i] = 0$ with $\partial_d\Pi_{n+1}(\boldsymbol{u}^i, d^i) \geq 0$, $\Delta d^i \geq 0$
- compute $Res_{stag} = \partial_u\Pi(\boldsymbol{u}^i, d^i)$

$(\boldsymbol{u}_{n+1}, d_{n+1}) \to (\boldsymbol{u}^i, d^i)$

output: solution $(\boldsymbol{u}_{n+1}, d_{n+1})$

SYMMETRIC LINEAR COMPLEMENTARITY PROBLEM once spatially discretized!

Projected Successive Over-Relaxation algorithm

SYMMETRIC LINEAR COMPLEMENTARITY PROBLEM

$$(\mathbf{Q}^i \Delta\hat{\mathbf{d}} + \mathbf{q}^i) \cdot \Delta\hat{\mathbf{d}} = 0$$

$$-(\mathbf{Q}^i \Delta\hat{\mathbf{d}} + \mathbf{q}^i) \leq 0$$

$$\Delta\hat{\mathbf{d}} \geq 0$$

$$\mathbf{Q}^i := \boldsymbol{\Psi}(\hat{\mathbf{u}}^i) + G_c \boldsymbol{\Phi}\,, \quad \mathbf{q}^i := \mathbf{Q}^i \hat{\mathbf{d}}_n - \boldsymbol{\psi}(\hat{\mathbf{u}}^i)$$

ELEMENT QUANTITIES

$$\boldsymbol{\Phi}^{(e)} := \int_{\Omega_e} \left(l_0^{-1} \, (\mathbf{N}_d^{(e)})^{\mathrm{T}} \mathbf{N}_d^{(e)} + l_0 \, (\mathbf{B}_d^{(e)})^{\mathrm{T}} \mathbf{B}_d^{(e)} \right) \mathrm{d}\Omega_e$$

$$\boldsymbol{\Psi}^{(e)}((\hat{\mathbf{u}}^{(e)})^i) := \int_{\Omega_e} 2 \left(\psi_V^+((\hat{\mathbf{u}}^{(e)})^i) + \psi_D((\hat{\mathbf{u}}^{(e)})^i) \right) (\mathbf{N}_d^{(e)})^{\mathrm{T}} \mathbf{N}_d^{(e)} \, \mathrm{d}\Omega_e$$

$$\boldsymbol{\psi}^{(e)}((\hat{\mathbf{u}}^{(e)})^i) := \int_{\Omega_e} 2 \left(\psi_V^+((\hat{\mathbf{u}}^{(e)})^i) + \psi_D((\hat{\mathbf{u}}^{(e)})^i) \right) (\mathbf{N}_d^{(e)})^{\mathrm{T}} \, \mathrm{d}\Omega_e$$

$$\mathbf{Q} = \mathbf{L} + \mathbf{D} + \mathbf{L}^{\mathrm{T}}$$

L := strictly lower triangular matrix (L_{rc}:=$Q_{r>c}$)

D := diagonal matrix (D_{rr}:=$Q_{r=c}$)

Algorithm 3.2 [Mangasarian, JOTA 1977]

$$\Delta d_r^k = \left\langle \Delta d_r^{k-1} - D_{rr}^{-1} \left[Q_{rc} \, \Delta d_c^{k-1} + q_r + L_{rc} \, (\Delta d_c^k - \Delta d_c^{k-1}) \right] \right\rangle_+$$

- ✓ irreversibility enforced componentwise in strong form *via* the Macaulay bracket operator
- ✓ explicit algorithm due to the strictly lower triangular format of matrix L

SEN specimen under shear loading
Global Response

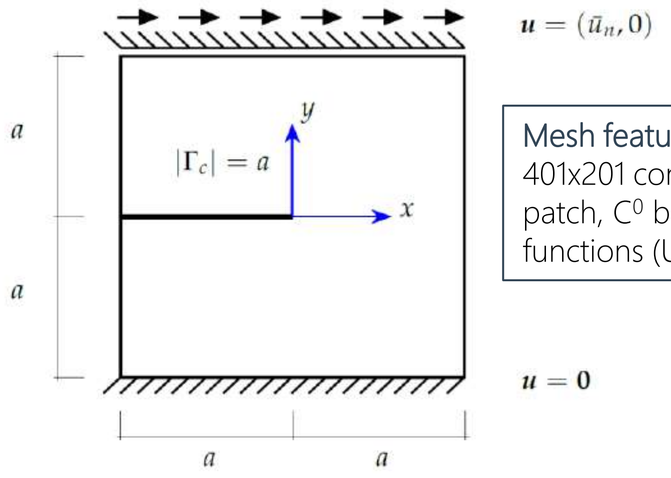

Mesh features: 2 patches, 401x201 control points per patch, C^0 bilinear shape functions (UOS)

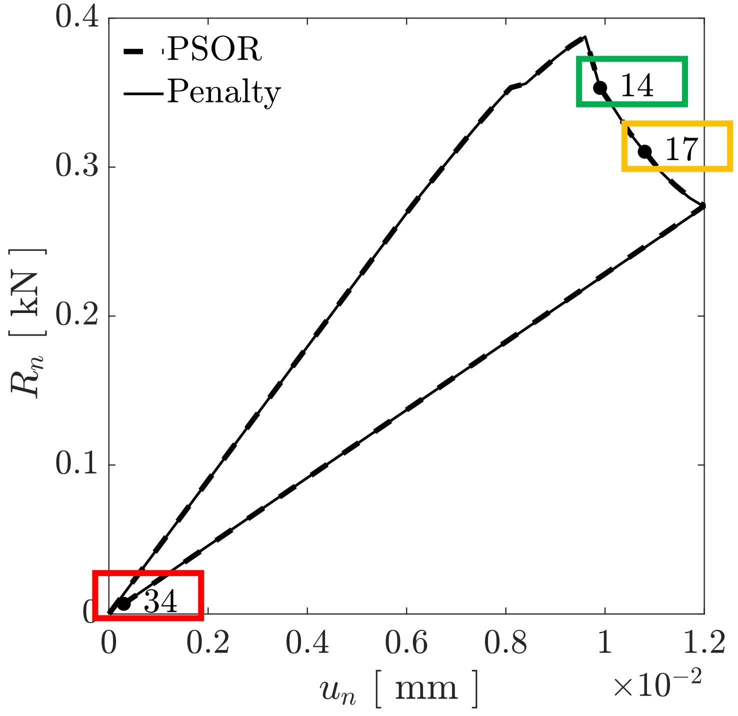

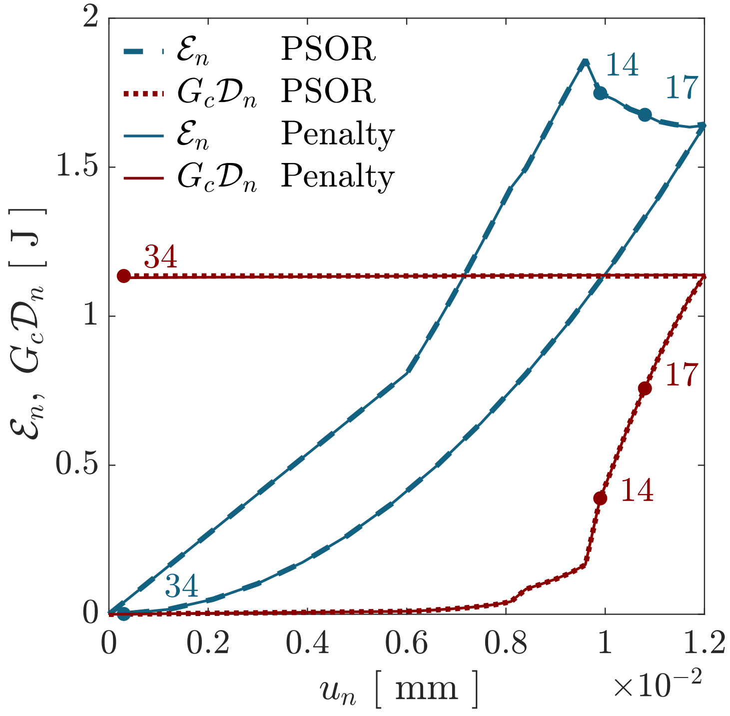

$TOL_{staggered}$	TOL_{PSOR}	$TOL_{penalty}$	$TOL_{NR,u}$
[kJ]	[-]	[-]	[kJ]
10^{-7}	10^{-4}	10^{-4}	10^{-9}

Adopted tolerances (UOS)

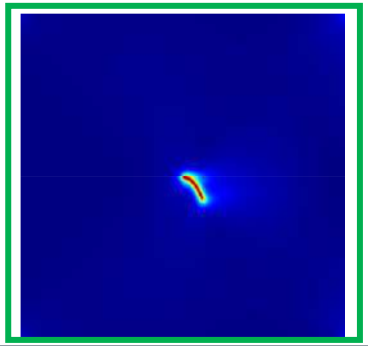

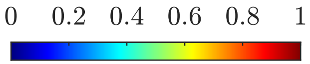

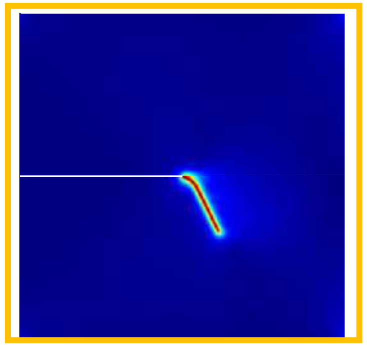

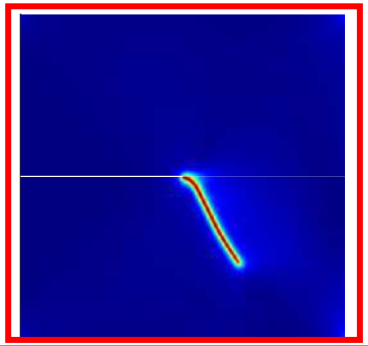

Possible alternative criteria for the staggered scheme

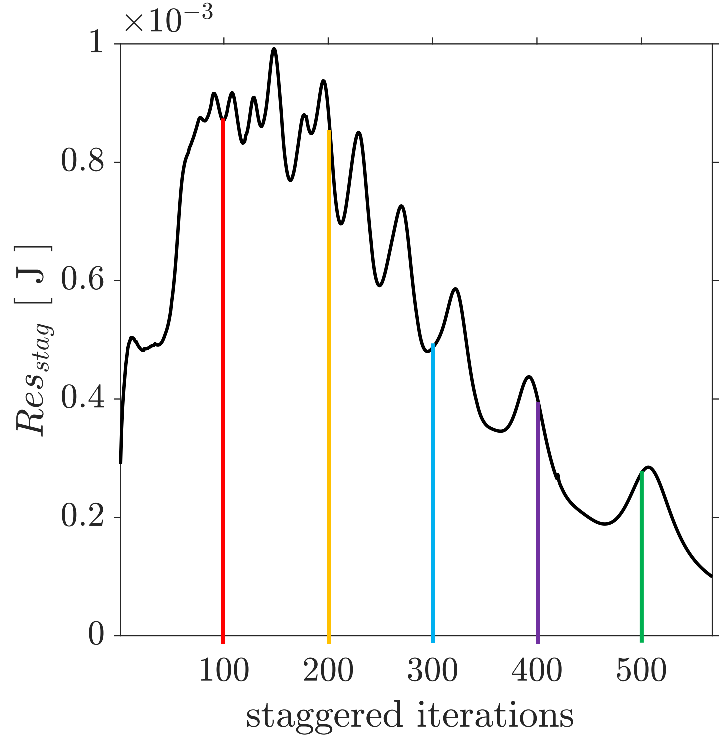

STEP 14

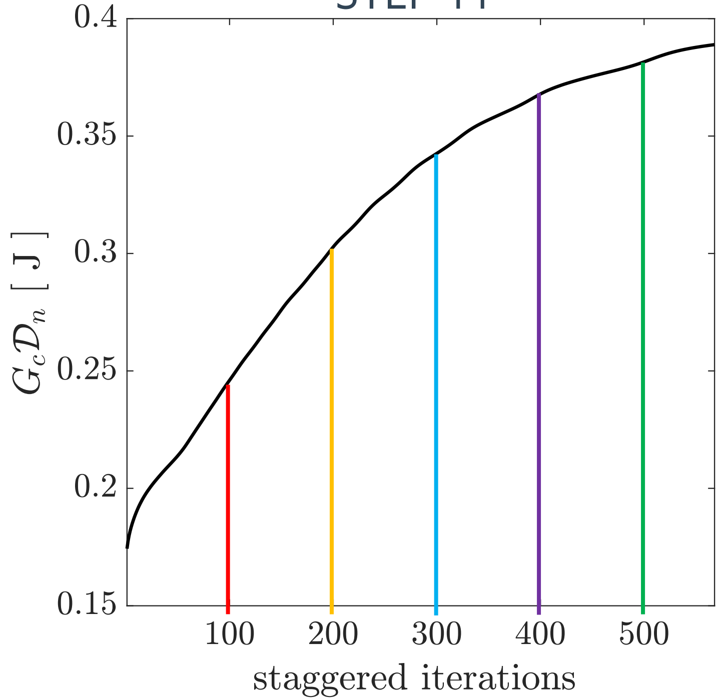

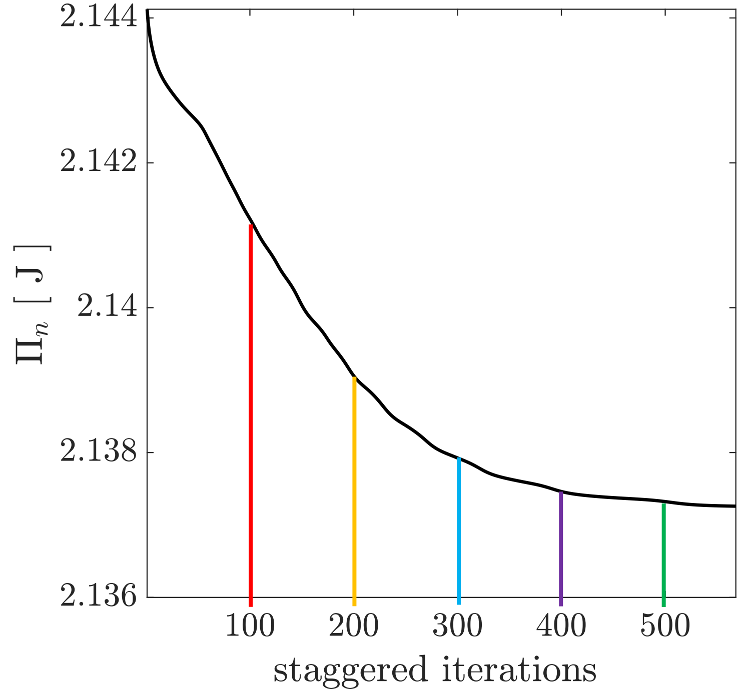

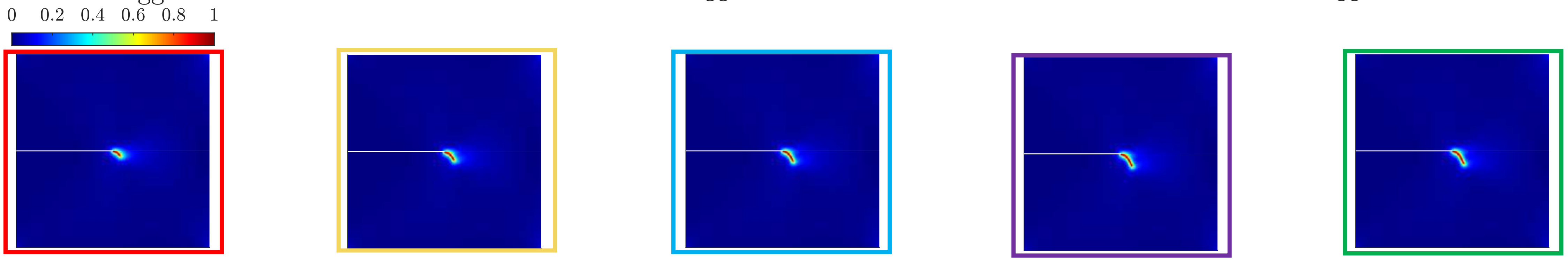

SEN specimen under shear loading

Time performance

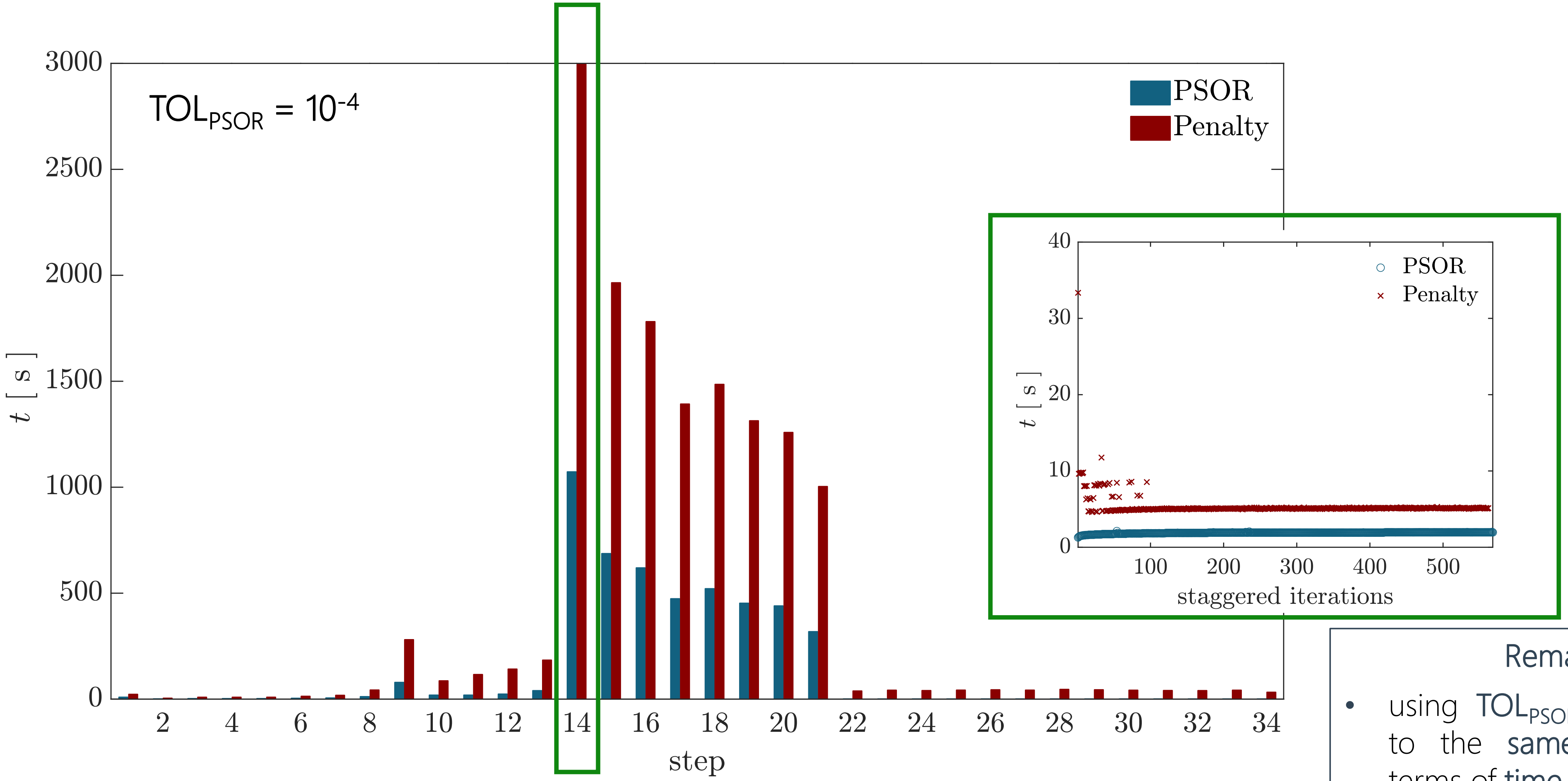

Remark

- using TOL$_{PSOR}$ = 10^{-6} leads to the same behavior in terms of time performance

L-shaped panel

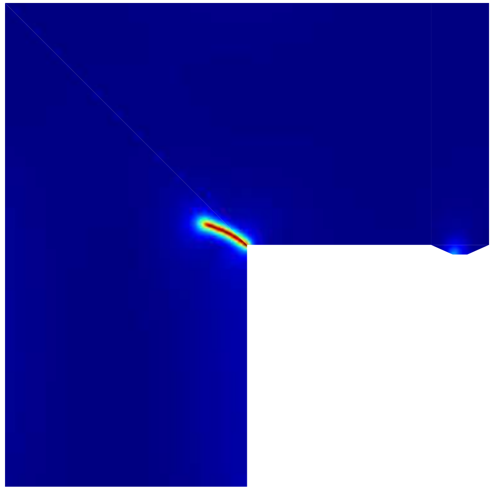

Phase-field solution at step 24

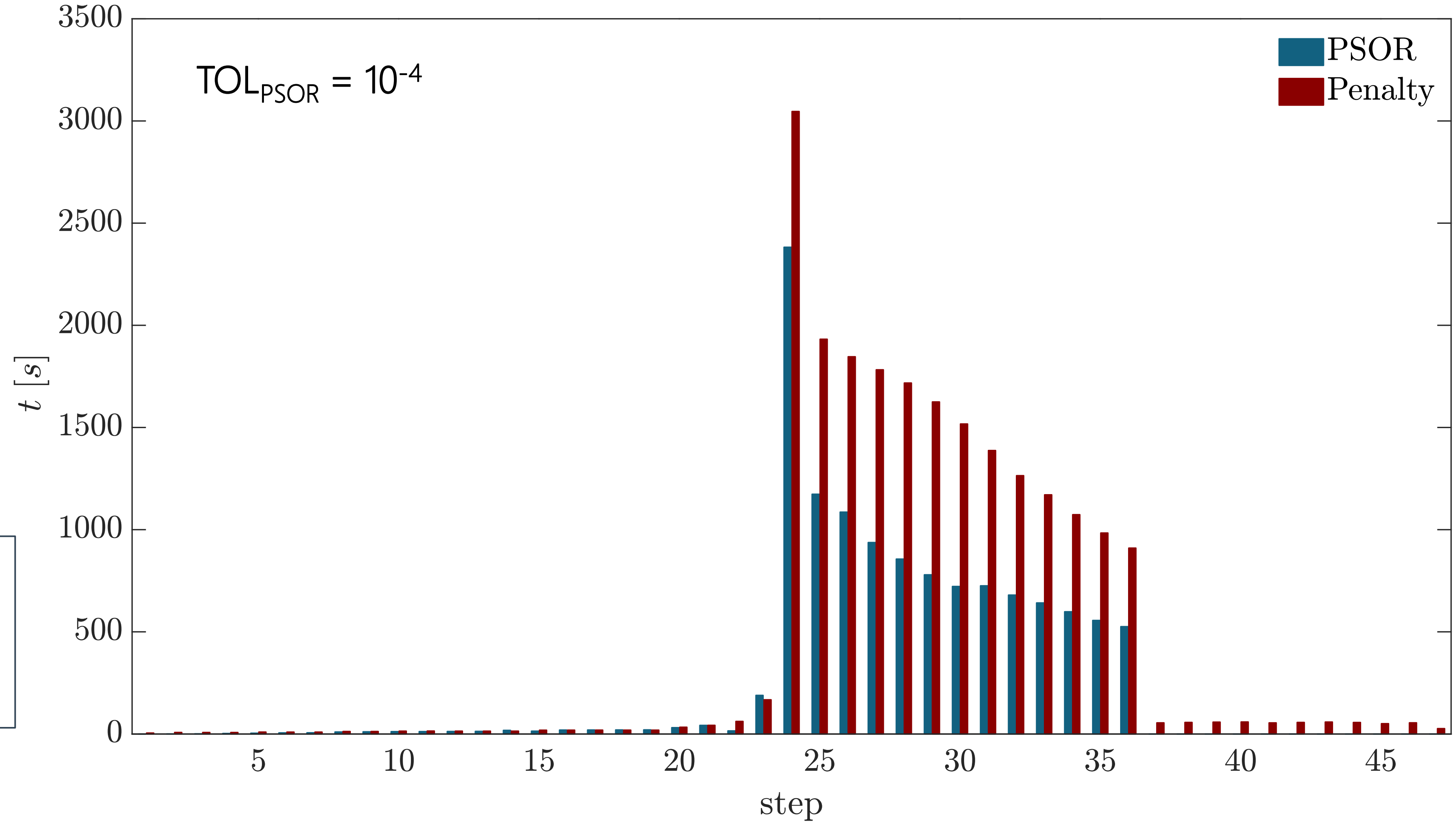

Remark

- using TOL$_{PSOR}$ = 10^{-6} is more computationally demanding for the PSOR method

SEN specimen under shear loading
Preliminary C^1 quadratic results

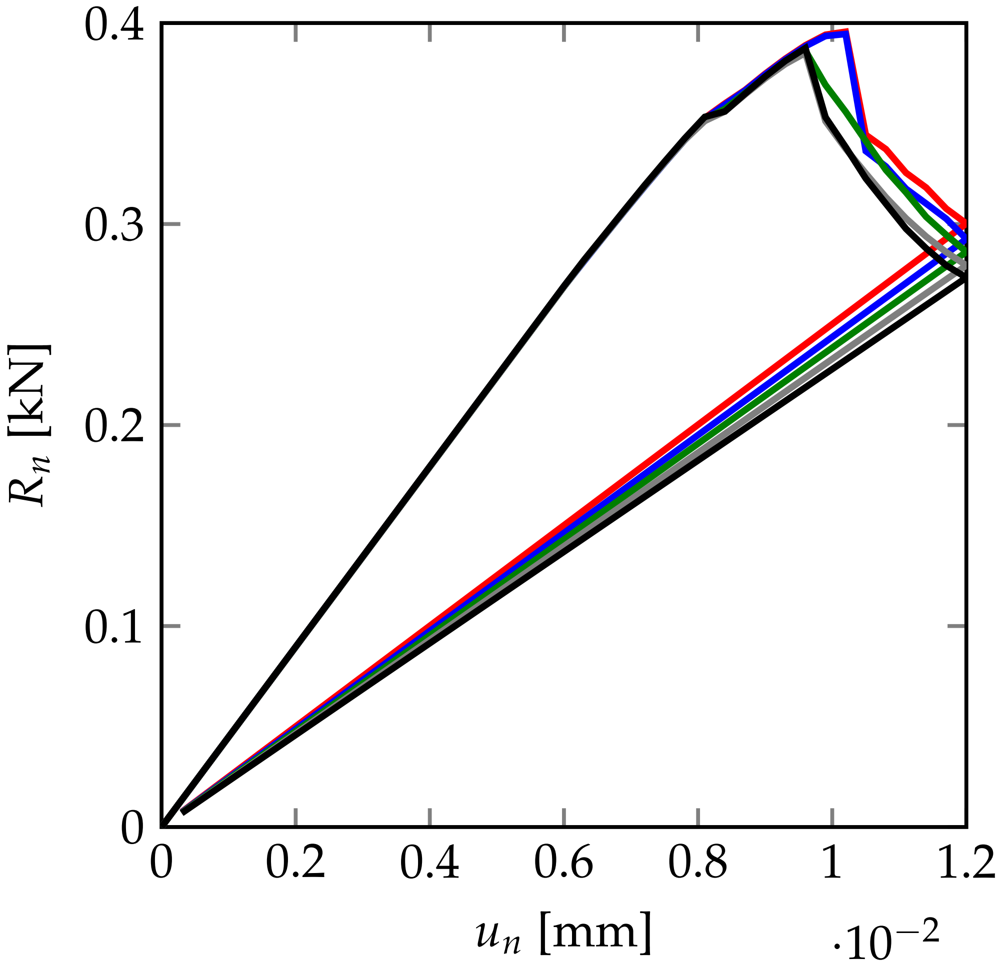

Remarks

- PSOR algorithm can be used also with higher-order, higher-continuity methods
- reducing TOL_{stag} does not yield a significant improvement in terms of solution accuracy
- the mesh resolution of the internal length is more relevant than the regularity of the B-spline approximation

PSOR 201x202 elements $TOL^{(1)}_{stag} = 10^{-7}$ kJ
PSOR 201x202 elements $TOL^{(2)}_{stag} = 10^{-10}$ kJ
PSOR 271x342 elements $TOL^{(1)}_{stag} = 10^{-7}$ kJ
PSOR 401x402 elements $TOL^{(1)}_{stag} = 10^{-7}$ kJ
Penalty 400x400 elements $TOL^{(1)}_{stag} = 10^{-7}$ kJ

A. Marengo, AP, M. Negri, U. Perego, and A. Reali, A rigorous and efficient explicit algorithm for irreversibility enforcement in phase-field finite element and isogeometric modeling of brittle crack propagation, status: submitted.

Outline

- Motivation
- Cost-effective IgA strategies to model composite structures
- An explicit algorithm for irreversibility enforcement in phase-field modeling of crack propagation
- Towards novel IgA methods for fluid-structure interaction problems
- Conclusions and Future works

Motivation

- Fluid-structure interaction (FSI) problems may involve extremely **complex discretizations** due to **the joint evolution of the fluid-solid interface**

- Typically addressed by **partitioned solution strategies/staggered schemes** which involve **sub-problem-dependent** discretizations
  - ✓ crucial to reduce the number of DOFs and increase the accuracy of the exchanged information
  - × non-matching interface discretizations

- **Spatial coupling strategies** of non-matching interface discretizations

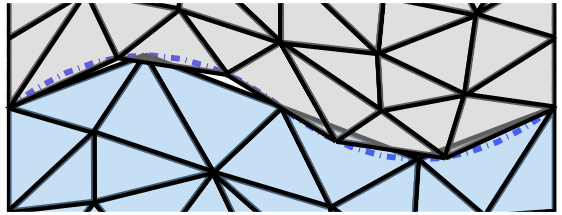

SFEM/SFEM

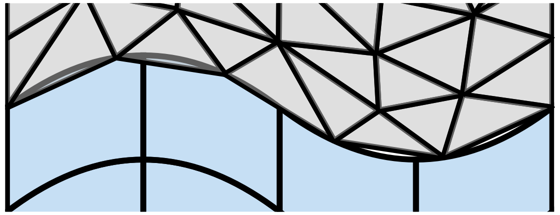

SFEM/IgG

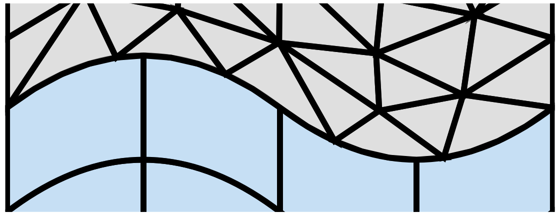

NEFEM/IgG

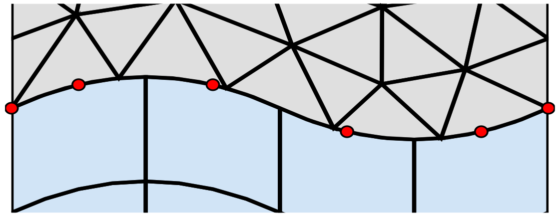

NEFEM/IgC

Motivation

- Fluid-structure interaction (FSI) problems may involve extremely **complex discretizations** due to **the joint evolution of the fluid-solid interface**

- Typically addressed by **partitioned solution strategies/staggered schemes** which involve **sub-problem-dependent** discretizations
  - ✓ crucial to reduce the number of DOFs and increase the accuracy of the exchanged information
  - × non-matching interface discretizations

- **Spatial coupling strategies** of non-matching interface discretizations

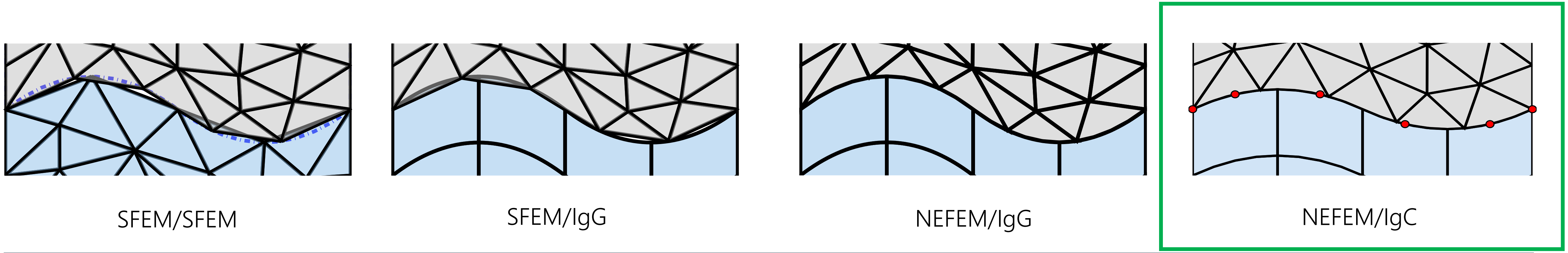

Problem statement

Fluid problem (Eulerian viewpoint)

Balance laws for mass and linear momentum (incompressible material)

$$\nabla \cdot \boldsymbol{v} = 0 \quad \text{in } \Omega_x \ \forall t \in [0,T]$$

$$\rho^f \left(\frac{\partial \boldsymbol{v}}{\partial t} + \boldsymbol{v} \cdot \boldsymbol{\nabla} \boldsymbol{v} - \mathbf{f} \right) - \boldsymbol{\nabla} \cdot \mathbf{T} = \mathbf{0} \quad \text{in } \Omega_x \ \forall t \in [0,T]$$

Total stress tensor $\mathbf{T}(\boldsymbol{v}, p) = -p\mathbf{I} + 2\mu^f \mathbf{D}(\boldsymbol{v})$

Strain rate tensor $\mathbf{D}(\boldsymbol{v}) = \frac{1}{2}\left(\boldsymbol{\nabla}\boldsymbol{v} + (\boldsymbol{\nabla}\boldsymbol{v})^{\mathrm{T}}\right)$

B.C's

$$\boldsymbol{v} = \boldsymbol{h} \quad \text{on } (\Gamma_x)_D$$

$$\mathbf{T} \cdot \boldsymbol{n} = \boldsymbol{t}^f \quad \text{on } (\Gamma_x)_N$$

I.C.

$$\boldsymbol{v}(\mathbf{x}, 0) = \boldsymbol{v}^0(\mathbf{x}) \quad \text{in } \Omega_x \text{ at } t = 0$$

Solid problem (Lagrangian viewpoint)

Balance of linear momentum

$$\rho^s \frac{d^2 \boldsymbol{u}}{dt^2} = \boldsymbol{\nabla}_{\mathbf{X}} \cdot (\mathbf{FS}) + \boldsymbol{B} \quad \text{in } \Omega_X \ \forall t \in [0,T]$$

Deformation gradient $\mathbf{F} = \frac{\partial \mathbf{x}}{\partial \mathbf{X}}$

Green-Lagrange strain $\mathbf{E} = \frac{1}{2}\left(\mathbf{F}^{\mathrm{T}}\mathbf{F} - \mathbf{I}\right)$

PK2, KSV $\mathbf{S} = \lambda^s \mathrm{tr}(\mathbf{E})\mathbf{I} + 2\mu^s \mathbf{E}$

B.C's

$$\boldsymbol{u} = \boldsymbol{g} \quad \text{on } (\Gamma_X)_D$$

$$(\mathbf{FS}) \cdot \mathbf{N} = \boldsymbol{t}^s \quad \text{on } (\Gamma_X)_N$$

I.C's

$$\boldsymbol{u}(\mathbf{X}, 0) = \boldsymbol{u}^0 \quad \text{in } \Omega_X \text{ at } t = 0$$

$$\frac{d\boldsymbol{u}(\mathbf{X}, 0)}{dt} = \boldsymbol{v}^0 \quad \text{in } \Omega_X \text{ at } t = 0$$

Coupling conditions at the FSI interface

Kinematic continuity

$$\mathbf{x}^f = \mathbf{x}^s$$

$$\boldsymbol{v}^f = \boldsymbol{v}^s$$

Dynamic continuity

$$\mathbf{T} \cdot \boldsymbol{n}^f = \boldsymbol{\sigma} \cdot \boldsymbol{n}^s$$

on Γ^{fsi}

$$\boldsymbol{t}^s = (\mathbf{FS}) \cdot \mathbf{N} = \det(\mathbf{F})(\mathbf{T}\mathbf{F}^{-\mathrm{T}}) \cdot \mathbf{N}$$

Problem statement

Fluid problem (Eulerian viewpoint)

Balance laws for mass and linear momentum (incompressible material)

$$\nabla \cdot \boldsymbol{v} = 0 \quad \text{in } \Omega_x \ \forall t \in [0,T]$$

$$\rho^f \left(\frac{\partial \boldsymbol{v}}{\partial t} + \boldsymbol{v} \cdot \nabla \boldsymbol{v} - \mathbf{f} \right) - \nabla \cdot \mathbf{T} = \mathbf{0} \quad \text{in } \Omega_x \ \forall t \in [0,T]$$

Total stress tensor $\mathbf{T}(\boldsymbol{v}, p) = -p\mathbf{I} + 2\mu^f \mathbf{D}(\boldsymbol{v})$

Strain rate tensor $\mathbf{D}(\boldsymbol{v}) = \frac{1}{2}\left(\nabla \boldsymbol{v} + (\nabla \boldsymbol{v})^{\mathrm{T}}\right)$

B.C's

$$\boldsymbol{v} = \boldsymbol{h} \quad \text{on } (\Gamma_x)_D$$

$$\mathbf{T} \cdot \boldsymbol{n} = \boldsymbol{t}^f \quad \text{on } (\Gamma_x)_N$$

I.C.

$$\boldsymbol{v}(\mathbf{x}, 0) = \boldsymbol{v}^0(\mathbf{x}) \quad \text{in } \Omega_x \text{ at } t = 0$$

Solid problem (Lagrangian viewpoint)

Balance of linear momentum

$$\rho^s \frac{d^2 \boldsymbol{u}}{dt^2} = \nabla_{\mathbf{X}} \cdot (\mathbf{F}\mathbf{S}) + \boldsymbol{B} \quad \text{in } \Omega_X \ \forall t \in [0,T]$$

Deformation gradient $\mathbf{F} = \frac{\partial \mathbf{x}}{\partial \mathbf{X}}$

Green-Lagrange strain $\mathbf{E} = \frac{1}{2}\left(\mathbf{F}^{\mathrm{T}}\mathbf{F} - \mathbf{I}\right)$

PK2, KSV $\mathbf{S} = \lambda^s \mathrm{tr}(\mathbf{E})\mathbf{I} + 2\mu^s \mathbf{E}$

B.C's

$$\boldsymbol{u} = \boldsymbol{g} \quad \text{on } (\Gamma_X)_D$$

$$(\mathbf{F}\mathbf{S}) \cdot \mathbf{N} = \boldsymbol{t}^s \quad \text{on } (\Gamma_X)_N$$

I.C's

$$\boldsymbol{u}(\mathbf{X}, 0) = \boldsymbol{u}^0 \quad \text{in } \Omega_X \text{ at } t = 0$$

$$\frac{d\boldsymbol{u}(\mathbf{X}, 0)}{dt} = \boldsymbol{v}^0 \quad \text{in } \Omega_X \text{ at } t = 0$$

Linearization [Kruse et al., CMAME 2015]

Generalized-α method [Chung and Hulbert, JAM 1993]

Coupling conditions at the FSI interface

Kinematic continuity

$$\mathbf{x}^f = \mathbf{x}^s$$

$$\boldsymbol{v}^f = \boldsymbol{v}^s$$

Dynamic continuity

$$\mathbf{T} \cdot \boldsymbol{n}^f = \boldsymbol{\sigma} \cdot \boldsymbol{n}^s$$

on Γ^{fsi}

$$\boldsymbol{t}^s = (\mathbf{F}\mathbf{S}) \cdot \mathbf{N} = \det(\mathbf{F})(\mathbf{T}\mathbf{F}^{-\mathrm{T}}) \cdot \mathbf{N}$$

Temporal Coupling

STAGGERED ALGORITHM

for $k = 1, \ldots$ until convergence

1. *Prediction step:* Prescribe $(\boldsymbol{u}_1^s)^{n+1}$ based on the total stress tensor $\mathbf{T}_n$ at the previous time step t^n.

2. *Dirichlet step:* Deform the fluid grid according to $(\boldsymbol{u}_k^s)^{n+1}$, solve the fluid problem for $(\boldsymbol{v}_k)^{n+1}, (p_k)^{n+1}$ and compute the total stress $(\mathbf{T}_k)^{n+1}$.

3. *Neumann step*: Solve the solid problem for $(\boldsymbol{u}_{k+1}^s)^{n+1}$ by imposing the tractions coming from the fluid problem. $(\boldsymbol{t}_k^s)^{n+1} = \det((\mathbf{F}_k)^{n+1})(\mathbf{T}_k)^{n+1}(\mathbf{F}_k^{-\mathrm{T}})^{n+1} \cdot \mathbf{N} \quad \text{on } \Gamma^{fsi}$

4. *Check convergence*: if $\left|\left|(\boldsymbol{u}_{k+1}^s)^{n+1} - (\boldsymbol{u}_k^s)^{n+1}\right|\right| < \epsilon$ proceed to the next time step, otherwise continue iterating with $k = k + 1$ and go to step 2.

end loop

Numerical validation

Turek-Hron FSI benchmark

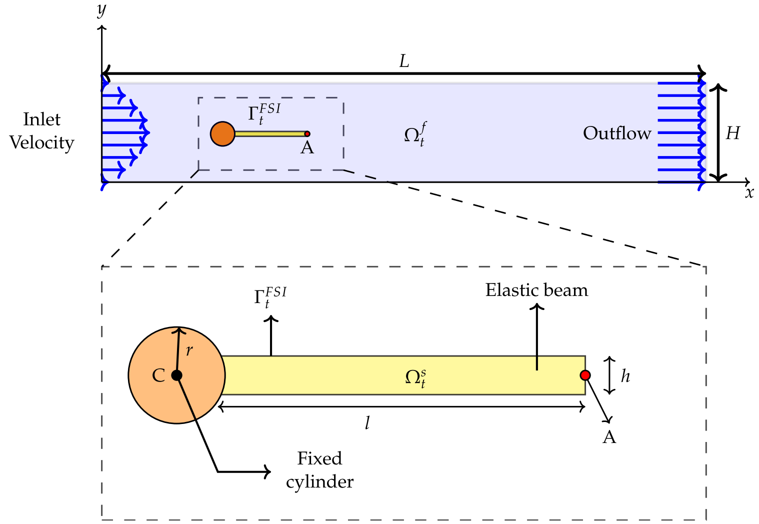

Geometry parameters	**Abbreviations**	**Value [m]**
Channel length	L	2.5
Channel width	H	0.41
Structure length	l	0.35
Structure thickness	h	0.02
Cylinder radius	r	0.05
Cylinder center position	C	(0.2,0.2)
Reference point (at $t = 0$)	A	(0.6,0.2)

Standalone structural test

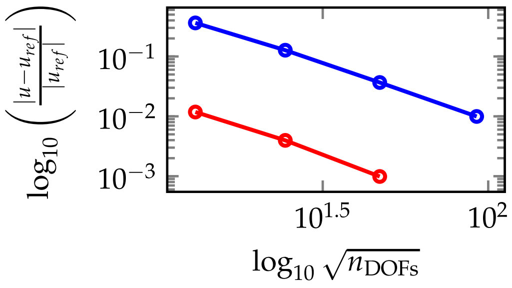

(a) linear elasticity

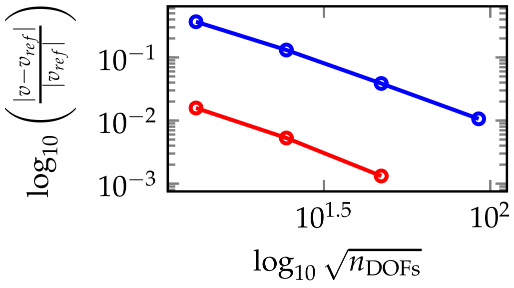

(b) nonlinear elasticity

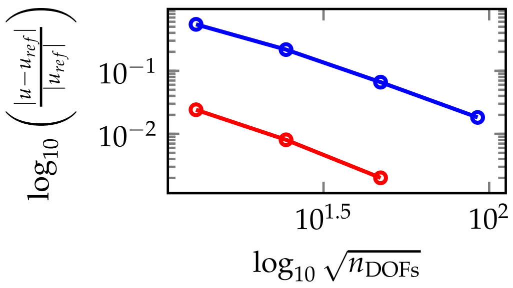

(c) linear elasticity

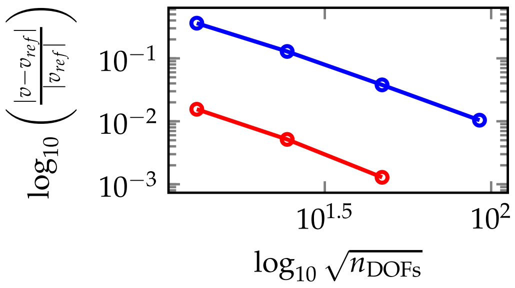

(d) nonlinear elasticity

Relative displacement error at the lower right corner of the beam for 17x5, 33x9, 65x17, and 129x33 control points vs. the square root of the total number of DOFs for each considered mesh: o IgG, o IgC .

Numerical validation

Steady FSI benchmark

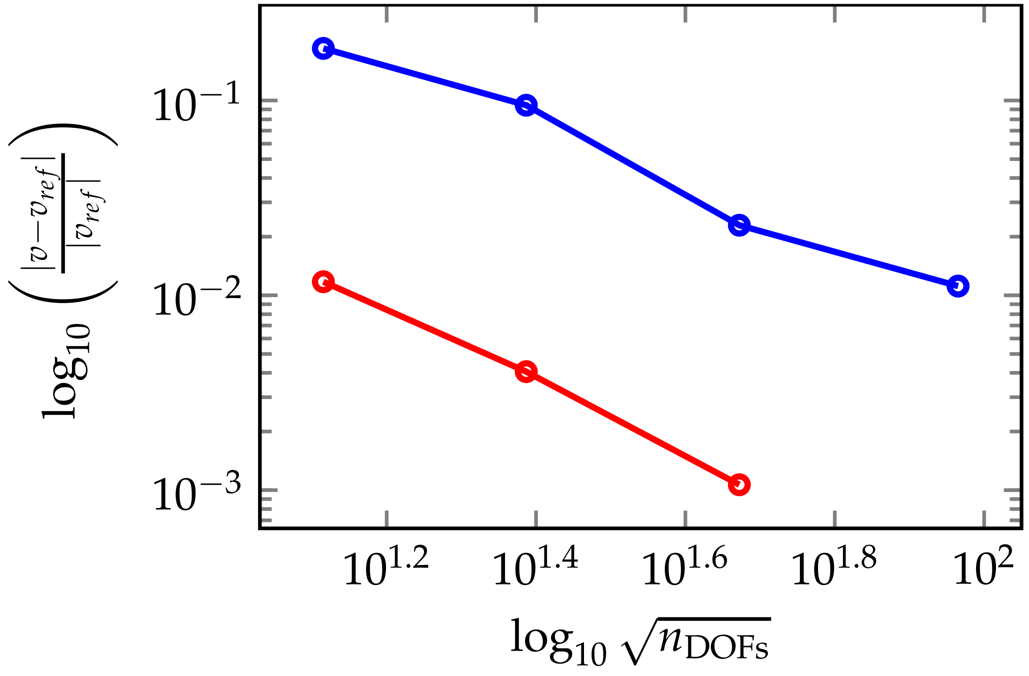

Relative displacement error at point A of the beam for 17x5, 33x9, 65x17, and 129x33 control points vs. the square root of the total number of DOFs for each considered mesh: ○ IgG, ○ IgC .

Unsteady FSI benchmark

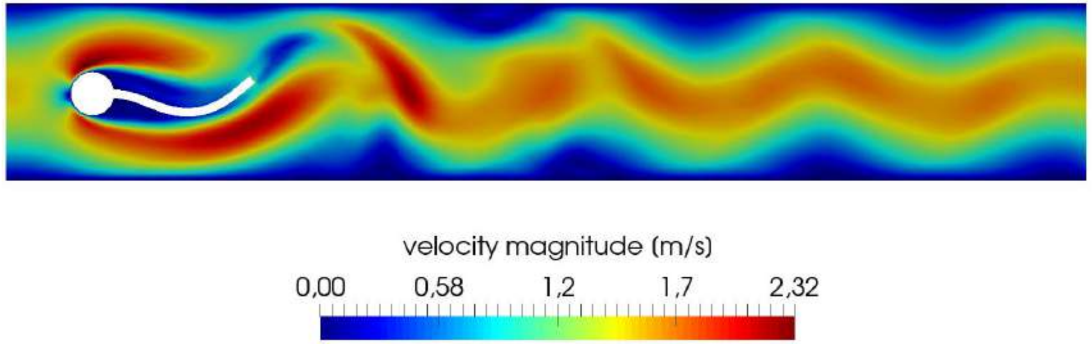

snapshot of the simulated flow field and beam deformation at t = 7.4 s

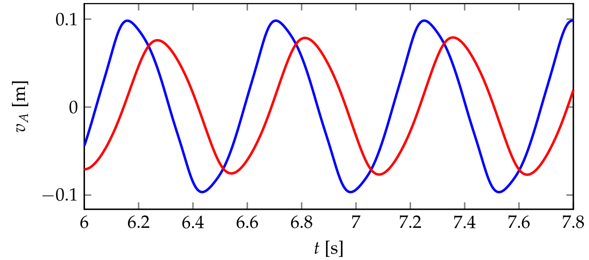

response of the vertical displacement for point A for a sampled time interval [6 s, 7.8 s]: ▬ NEFEM-IgG vs. ▬ NEFEM-IgC

N. Hosters, AP, N. Kubicki, A. Reali, S. Elgeti, M. Behr, Combining boundary-conforming finite elements and isogeometric collocation in the context of fluid-structure interaction, status: in preparation.

Outline

- Motivation
- Cost-effective IgA strategies to model composite structures
- An explicit algorithm for irreversibility enforcement in phase-field modeling of crack propagation
- Towards novel IgA methods for fluid-structure interaction problems
- Conclusions and Future works

Conclusions and Future works

Cost-effective IgA strategies to model composite structures

– Main results

- Novel stress recovery technique to simulate laminated composites (solid plates) behavior: displacement-based single-element IgA method combined with equilibrium equations direct integration relying on IgA shape functions higher continuity properties
- Extension to bivariate Kirchhoff plates (✓ antisymmetric cross-ply laminates; higher regularity demands w.r.t. the solid plate formulation)
- Extension to solid shells (local approach; ✓ doubly-curved solid shells)

– Future works

- Explore continuity requirements of the stress recovery (approach with 1st-order derivatives of out-of-plane stresses)
- Extension to bivariate shells
- Extension to inelastic problems is not trivial and *requires an iterative procedure*
- Extension to geometrically nonlinear problems

Conclusions and Future works

An explicit algorithm for irreversibility enforcement in phase-field modeling of crack propagation

– Main results

- Novel strategy featuring PSOR algorithm to rigorously and explicitly enforce irreversibility in finite element and IgA computations of phase-field brittle fracture
- Significant reduction in terms of elapsed time of the execution of the phase-field subroutine with respect to state-of-the art methods
- PSOR can be combined with an IgA discretization, considering a biquadratic C^1 approximation

An explicit algorithm for irreversibility enforcement in phase-field modeling of crack propagation

– Future works

- Explore higher-order models of fracture
- Extension to delamination and plasticity

Conclusions and Future works

Towards novel IgA methods for fluid-structure interaction problems

– Main results

- Novel coupling scheme for FSI problems: boundary-conforming finite elements (NEFEM) on the fluid side, IgC on the structural side, and a common spline representation of the fluid-solid interface
- Preliminary convergence tests assess attained coupling in the case of steady FSI simulations

Towards novel IgA methods for fluid-structure interaction problems

– Future works

- Further validation for transient FSI configurations
- Reduce the computational time for unsteady nonlinear case (i.e., explore higher orders for IgC, parallelization)

Dhanyavaad Merci Obrigado

Thank Grazie Gracias

Gracias you Kiitos

Danke Arigato Tak Xiè xie

Università degli Studi di Pavia
Facoltà di Ingegneria
PhD Program in Design, Modeling, and Simulation in Engineering
XXXIII ciclo

Advanced isogeometric methods with a focus on composite laminated structures

Alessia Patton

Pavia, April 20, 2021

Supervisor:
Prof. Alessandro Reali

Co-supervisor:
Dr. Guillermo Lorenzo